Occurrence of *Nigrospora* spp. as the predominant causal agents of leaf spot disease in Cavendish banana in banana plantations in Mindanao Island, Philippines

Short title: *Nigrospora* spp.: Major pathogens on Cavendish banana in Mindanao

Shunsuke Nozawa[1*], Yui Harada[1], Yoshiki Takata[1], Keiko Uchida[1], Mike Andre Malonzo[2], Reynaldo Valle[2], Sherman M. Chavez[3], Aniway F. Penalosa[3], Kyoko Watanabe[1*]

[1] School of Agriculture, Tamagawa University, Machida, Tokyo, Japan

[2] BaCaDM project of College of Agriculture, Tamagawa University, 6-1-1 Tamagawa-gakuen, Machida, Tokyo 194-8610, Japan

[3]Unifrutti Tropical Philippines, Inc., Km. 15, Panacan, Davao City 8000, Philippines

*Corresponding author:

E-mail: nozao802@gmail.com (N.S.) and wkyoko@agr.tamagawa.ac.jp (W.K.)

Abstract

Banana leaf diseases are a significant threat to Cavendish banana production. In the Philippines, the main disease has been diagnosed as Black sigatoka disease caused by *Pseudocercospora fijiensis* based on symptoms. However, our study showed that the main pathogen in Mindanao island, the largest banana-producing region in the Philippines, belongs to the genus *Nigrospora*, contradicting previous assumptions. We clarified the phylogenetic positions of 160 *Nigrospora* isolates based on molecular phylogenetic analyses using ITS, *β-tubulin*, and *tef1α* sequences, and compared their morphology with known species. Molecular phylogenetic and morphological analysis revealed that *Nigrospora* isolates comprised *N. chinensis*, *N. lacticolonia*, *N.* cf. *singularis*, *N. sphaerica*, *N. vesicularifera*, and a novel species, *N. nigrocolonia*. Pathogenicity tests on banana leaves confirmed that these species are pathogenic. Species other than *N. sphaerica* were for the first time reported as pathogens of banana leaf. The results of the fungicide sensitivity test using 14 fungicides, including pyrimethanil, spiroxamine, and tebuconazole, for the Sigatoka disease showed 100% inhibition of all isolates at 100 ppm of active ingredients. However, low-sensitivity isolates were observed for the remaining 11 fungicides. Our findings indicated the need for a comprehensive review of banana leaf disease prevention strategies.

Introduction

Banana is a cash crop in Southeast Asia, Africa, and Latin America, with an annual production of 1.51 million tons in 2023, making it the most produced fruit globally (FAOSTAT 2023). The Cavendish banana is the most widely traded and globally distributed variety among all banana cultivars. Cavendish is exported in significant quantities among the banana cultivars traded internationally. More than 20 million tons of Cavendish banana are exported. The leading exporters of Cavendish banana include Colombia, Costa Rica, Ecuador, Guatemala, and the Philippines, and its major importers are the European Union and United States.

Banana production is affected by diseases such as Fusarium wilt caused by *Fusarium* spp. [1,2], leaf blight by *F. saccari* and *Alternaria* jacinthicola [3,4]; leaf spots by *Colletotrichum* spp., *Pseudocercospora eumusae*, and *Nigrospora* shaerica [5–7]; and Sigatoka disease by *Pseudocercospora* spp. [8]. Among these diseases, Sigatoka disease is one of the most serious, causing an estimated 3% annual reduction in banana yield and economic losses of approximately 1.6 billion dollars annually [9]. The Sigatoka disease is caused by several *Pseudocercospora* spp.; black Sigatoka by *P. fijiensis*, and yellow Sigatoka by *P.* musae [10]. Among these diseases, *P. fijiensis* (black Sigatoka) is the most virulent and causes serious damage. Since its discovery in Fiji in 1964 [11], the disease has spread globally owing to its virulence and infectiousness, becoming one of the most serious threats to banana production.

The Philippines is the world's fifth-largest producer of bananas, with an annual output of approximately 5.9 million tons in 2023 (FAOSTAT 2023). Bananas are pivotal cash crops for export, with an estimated annual export volume of approximately 2 million tons. However, the country is grappling with a significant challenge: black Sigatoka disease, the management of which has necessitated substantial financial investments [10]. To address this issue, a leaf removal strategy was implemented to eliminate leaves exhibiting disease symptoms and maintain a minimum of five leaves per plant. This approach involves fungicide applications, sprayed approximately 50 to 70 times per year, to prevent disease transmission. According to the Banana Working Group of the Fungicide Resistance Action Committee (FRAC), the following fungicide groups are recommended for the control of Sigatoka disease: amines, anilinopyrimidines (APs), benzimidazoles (BCMs), demethylase inhibitors (DMIs), guanidines, multi-site inhibitors, N-Phenylcarbamates, Qi Inhibitors (QiIs), Qo Inhibitors (QoIs), Succinate Dehydrogenase Inhibitors (SDHIs), and Toluamides. Fungicide application incurs high annual costs and is the most expensive activity in banana production. However, there is a paucity of surveys conducted in the Philippines to investigate the emergence of new pathogens despite the presence of multiple diseases that can present spot symptoms similar to Sigatoka disease in the world [5,7,12].

Our study shows that *Nigrospora* spp., rather than *Pseudocercospora* spp., is the dominant pathogen on the island of Mindanao in the Philippines. This symptom closely resembles that of Sigatoka disease, as it causes the formation of brown to black spots with a yellow halo and the lesions expand along the leaf veins (Fig. 1). Consequently, locally, any disease exhibiting such symptoms is diagnosed as Sigatoka disease.

To provide basic information for control measures against this disease, which is mistakenly diagnosed as Sigatoka disease, we identified the pathogens belonging to the genus *Nigrospora* at the species level and conducted haplotype analysis. In addition, in vitro sensitivity tests were conducted to identify effective fungicides currently used to control black Sigatoka disease and hypothesize the potential emergence of resistant *Nigrospora* spp. isolates.

Results

Frequency of the genus *Nigrospora*

We obtained 217 isolates from diseased banana leaves. As a preliminary identification to determine the genus, a BLAST search of the ITS region in the NCBI database was conducted. A Basic Local Alignment (BLAST) search showed that our isolates consisted of 18 genera (Table 1). Out of 217 isolates, 160 belonged to the genus *Nigrospora*, which was the most frequently detected fungal genus. In addition, the genus *Nigrospora* was dominant at all the collection

locations. The proportions of *Nigrospora* were 96.6%, 70.2 %, 53.5 %, 92.9 %, 69 %, and 75% in Dabong-dabong, Little Panay, Panambon, Patag-Alanib, Tugbok, and Ula, respectively. We did not perform further analyses to identify the species of isolates that did not belong to the genus *Nigrospora*.

Phylogeny of isolates belonging to genus *Nigrospora*

To reveal the phylogenetic position of our isolates, we constructed molecular phylogenetic trees based on the combined data set of ITS, *β-tubulin*, and *tef1a* nucleotide sequences. The alignment length, number of variable sites, and number of parsimony-informative sites in the DNA data were 1,156, 545, and 461 bp, respectively (see Supplementary Data Set). The phylogenetic tree~~s~~ (Fig. 2; see Supplementary Data Set) showed that our isolates belonged to a clade comprised of *N. camelliae-sinensis* M. Wang & L. Cai and *N. singularis* M. Raza & L. Cai (30 isolates: 13.4% of all isolates; BPP/ML = 0.99/92, *N. chinensis* clade (1 isolate: 0.5% of all isolates; BPP/ML = 1.0/99), *N. lacticolonia* (118 isolates: 54.6% of all isolates; BPP/ML = 1.0/99), *N. nigrocolonia* Nozawa & Kyoko Watan. clade (9 isolates: 11.1% of all isolates; BPP = 1.0), *N. sphaerica* clade (1 isolate: 0.5% of all isolates; BPP/ML = 1.0/99), and *N. vesicularifera* clade (1 isolate: 0.5% of all isolates; BPP/ML = 1.0/99). Regarding the isolates belonging to a clade comprising of *N. camelliae-sinensis* and *N. singularis*, the evolutionary

distance between the isolates and the ex-type strain of *N. singularis* (CGMCC 3.19334) is closer than that to *N. camelliae-sinensis*. However, identifying the isolates collectively as *N. singularis* is not possible because *N. camelliae-sinensis* belongs within the same clade. Therefore, in this study, these isolates were treated as strains closely related to *N. singularis* and designated as *N.* cf. *singularis*. Although the clade comprising *N. camelliae-sinensis* and *N. singularis* warrants further taxonomic examination, in the present study, we focused on identification and therefore did not discuss this limitation.

The phylogenetic positions of the clades to which the isolates belong are as follows. *N. chinensis* clade neighbored *N. humicola* Qin Yang & Ning Jiang (BPP/ML = 1.0/99), *N. lacticolonia* clade neighbored *N. osmanthi* Mei Wang & L. Cai (BPP = 0.99/86), *N. nigrocolonia* clade, a new lineage, neighbored a clade comprising *N. cooperae* Y.P. Tan, Bishop-Hurley, Bransgr. & R.G. Shivas, *N. guilinensis* Mei Wang & L. Cai, *N. lacticolonia* Mei Wang & L. Cai clade, *N. marylouisemclawsiae* Y.P. Tan, Ryley & Bishop-Hurley, and *N. osmanthi*, *N. sphaerica* clade neighbored *N. brasiliensis* A.C.Q. Brito, C. Conforto & A.R. Machado (BPP/ML = 1.0/99), and *N. vesicularifera* clade neighbored *N. saccharicola* M. Raza & L. Cai (BPP/ML = 0.99/99).

Phylogenetic analyses were conducted based on three DNA regions (ITS, β-tubulin, and *tef1a*; Supplementary Figure 1; see Supplementary Data Set) independently. Among the isolates,

thirty strains identified as *N.* cf. *sphaerica* formed a monophyletic clade with the reference strains of *N. camelliae-sinensis*, *N. falsivesicularis* M. Raza & L. Cai, and *N. pyriformis* Mei Wang & L. Cai in the phylogenetic tree based on ITS region (ITS tree; BPP < 0.95). In contrast, these strains formed a strongly supported monophyletic clade (BPP = 1.0) with *N. camelliae-sinensis*, *N. pyriformis*, and *N. sphaerica* (Sacc.) E.W. Mason in the phylogenetic tree based on the *β-tubulin* region (*β-tubulin* tree; Supplementary Figure 2). In the phylogenetic tree based on *tef1a* (*tef1a* tree; Supplementary Figure 3), although posterior probabilities were not indicated, the isolates formed a monophyletic group with *N. singularis*.

The isolate identified as *N. chinensis* Mei Wang & L. Cai consistently formed a well-supported monophyletic clade (BPP = 1.0 for all loci) with the reference strains of *N. chinensis*, including the ex-type strain, across all ITS, β-tubulin, and *tef1a* trees (Supplementary Figure 1, 2, 3). The isolates identified as *N. lacticolonia* formed a monophyletic clade with *N. osmanthi* and *N. vesicularifera* M. Raza & L. Cai in the ITS tree; however, they clustered with the reference strains of *N. lacticolonia* (including the ex-type strain) in both the β-tubulin and *tef1α* trees (BPP = 1.0/0.83: β-tubulin/*tef1a*). Similarly, the isolate identified as *N. sphaerica* formed a monophyletic clade with the reference *N. sphaerica* (including the ex-type strain) across all loci (BPP = 0.93/1.0/1.0 for ITS/*β-tubulin*/*tef1a*). The isolate identified as *N. vesicularifera* clustered with the reference strains of *N. vesicularifera* (including the ex-type strain) in both the β-tubulin

and *tef1a* trees (BPP = 1.0/1.0), while in the ITS tree, it formed a monophyletic group with both *N. vesicularifera* and *N. saccharicola* (BPP = 1.0). Although species-level resolution was not always clearly delineated in phylogenies based on single locus, all isolates were positioned within clades closely related to the corresponding identified species. Furthermore, the newly established species *N. nigrocolonia* was independent from any known species in all phylogenetic trees (BPP = 1.0/1.0/1.0: ITS/*β-tubulin* /*tef1a*).

Focusing on isolation frequency at each collection site, *N. lacticolonia* was the most frequently isolated species in Little panay, Panambon, Tugbok, and Ula. Meanwhile, *N. singuralis* M. Raza & L. Cai was the most frequently isolated species from Dabong-dabong and Patag-Alanib (Fig. 3a, b).

Taxonomy

Nigrospora nigrocolonia Nozawa & Kyoko Watan., sp. nov. (Fig. 4.; Supplementary Figure 4)

MycoBank no: MB 858325.

Culture characteristics: Colonies on PDA reached 90 mm in diameter. After 5 days of incubation at 25 ± 0.5 °C, the colonies had smooth margins, initially white to whitish cream with abundant cottony aerial mycelia; the reverse was initially whitish cream (Fig. 4a, b). With age, the colonies on the surface became grayish, and dark olive-to-black on the reverse (Fig. 4c, d).

Asexual morph on SNA: Hyphae are hyaline to brown, highly-branched, septate, smooth, and 2.2–4.8 (mean ± SD = 3.1±0.1, n = 30) μm wide. Conidiophores are micronematous or semi-macronematous, flexuous, olivaceous or brown, smooth (Fig. 4e), measuring 5.1–10.6×2.5–4.3 μm (mean ± SD = 8.5±1.2×3.3±0.4, n = 4), frequently reduced to conidiogenous cells (Fig. 4e-g). Conidiogenous cells are aggregated in clusters or dispersed on hyphae, monoblastic, determinate, variable in shape, mostly subspherical to cylindrical, and olivaceous or brown, measuring 5.4–15.2×5.9–10.8 μm (mean ± SD = 8.7±0.3×7.9±0.2, n = 30). Conidia are solitary, aseptate, globose 13.2–18.7×14–18 (mean ± SD = 16.3±0.2×16.5±0.2, n = 30), and subglobose to ellipsoidal 14.4–19.2×11.7–15 (mean ± SD = 16.2±0.2×13.1±0.2, n = 30) (Fig. 4e-g). No chlamydospores were observed in this study. Sexual morphs were not observed.

Etymology: Specific epithet refers to the black coloration of the colony on the back.

Type: Dried culture specimen grown on SNA (TAP H-24N202, holotype); ex-type strain TAP24N202 isolated from diseased leaf of *Musa acuminata*, in Patag-Alanib, Lantapan, Bukidnon, Philippines, on December 11, 2024, isolated by Shunsuke Nozawa. The holotype specimen and ex-type strain were deposited in the culture collection of Tamagawa University, Japan. The GenBank accession numbers for the type strain of Nigrospora nigrocolonia are as follows: ITS: LC868094, *β-tubulin*: LC868147, and *tef1a*: LC868200.

Note: *N. nigrocolonia* forms a well-supported clade as a neighbor of a clade comprising *N. aurantiaca*, *N. cooperae*, *N. falsivesicularis*, *N. guilinensis*, *N. lacticolonia*, *N. marylouisemclawsiae*, *N. osmanthi*, *N. stoneae*, and *N. vesicularis* in the phylogenetic tree based on cancate. The holotype of *N. nigrocolonia* exhibited sequence differences with other *Nigrospora* species as follows: *N. aurantiaca* CGMCC 3.18130 showed ITS 1.1%, *β-tubulin* 12.4%, and *tef1a* 20.1%; *N. cooperae* BRIP 72440a showed ITS 1.9%, β-*tubulin* 13.0%, and *tef1a* 21.1%; *N. falsivesicularis* CGMCC3.19678 showed ITS 2.4%, *β-tubulin* 12.3%, and *tef1a* 21.4%; *N. guilinensis* CGMCC 3.18124 showed ITS 1.6%, β-tubulin 11.7%, and *tef1a* 20.5%; *N. lacticolonia* CGMCC 3.18123 showed ITS 1.6%, *β-tubulin* 9.0%, and *tef1a* 20.7%; *N. marylouisemclawsiae* BRIP 74865b showed ITS 1.3%, *β-tubulin* 9.0%, and *tef1a* 20.4%; *N. osmanthi* CGMCC 3.18126 showed ITS 1.6%, *β-tubulin* 10.0%, and *tef1a* 19.0%; *N. stoneae* BRIP 75022a showed ITS 1.1%, *β-tubulin* 15.7%, and *tef1a* 20.3%; and *N. vesicularis* CGMCC 3.18128 showed ITS 1.3%, *β-tubulin* 12.1%, and *tef1a* 20.6%.

N. nigrocolona differed from related species in exhibiting dark olivaceous conidiogenous cells upon maturation. The species is further distinguished by its conidial size. The conidial size of *N. nigrocolonia* was notably bigger—measuring 13.2–18.7×14–18 (mean ± SD = 16.3±0.2×16.5±0.2)—than those of *N. aurantiaca* (mean ± SD = 14.82 ± 0.79×11.78 ± 1.07 µm), *N. cooperae* (10–12.5×8.5–10.5 µm), *N. falsivesicularis* (mean ± SD = 13.62 ± 1.8 µm), *N.*

guilinensis (mean ± SD = 12.46 ± 0.62 × 9.69 ± 0.71 µm), *N. lacticolonia* (mean ± SD = 14.36 ± 1.04 µm), *N. osmanthi* (mean ± SD = 14.87 ± 0.63 µm), and *N. vesicularis* (mean ± SD = 14.8 ± 0.76 µm). Morphological data for *N. marylouisemclawsiae* and *N. stoneae* are currently unavailable and were therefore excluded from conidial comparisons.

In addition to the type strain identified as *N. nigrocolonia*, the following isolates—TAP24N222, TAP24N224, TAP24N229, TAP24N232, TAP24N237, TAP24N246, TAP24N250, and TAP24N252—have been deposited in the Tamagawa University Mycological Bio-bank of Plant Diseases.

Morphological descriptions of isolates

In this section, species other than *N. nigrocolonia* isolated in this study are described. For species from which multiple strains were obtained, one strain was randomly selected for morphological characterization.

Nigrospora cf. *singularis*: Isolate no. TAP24N068: Culture characteristics: Colonies on PDA reached 90 mm in diameter. After 4 days of incubation at 25 ± 0.5 °C, the colonies had smooth margins and were white to whitish gray with abundant cottony aerial mycelia; the reverse was initially whitish cream (Fig.5a, b). Asexual morph on SNA: Hyphae are hyaline to pale brown, branched, septate, smooth, and 1.2–5.1 (mean±SD = 2.4±0.13, n = 30) µm wide.

Conidiophores are micronematous or semi-macronematous, flexuous, hyaline, and smooth. Conidiogenous cells are dispersed on hyphae, monoblastic, determinate, variable in shape, mostly subspherical to oblate, hyaline, measuring 6.4–16.1×6.4–17.3 (mean±SD = 9.4±0.41×8.1±0.35, n = 30) in size (Fig. 5c, d). Conidia are solitary, aseptate, and subglobose to ellipsoidal 9.8–13×9–13 (mean±SD = 11.6±0.18×11±0.22, n = 30; Fig.4c, d). No chlamydospores were observed in this study. Sexual morphs were not observed. The size of the conidia of this strain closely matched the original description of *N. singularis* (CGMCC 3.19334) [13]: 9.5–13 × 11–15 (mean ± SD = 11.2 ± 1.11 × 13.4 ± 1.12) μm.

N. chinensis: Isolate no. TAP24N249: Culture characteristics: Colonies on PDA reached 90 mm in diameter. After 7 days of incubation at 25 ± 0.5 °C, the colonies had smooth margins and were white to whitish cream, with abundant cottony aerial mycelia. the reverse was whitish gray to pale brown (Fig. 6a, b). Asexual morph on SNA: Hyphae are hyaline to pale brown, highly-branched, septate, smooth, and 1.5–4.6 (mean±SD = 2.7±0.14, n = 30) μm wide. Conidiophores are micronematous or semi-macronematous, flexuous, hyaline, smooth, frequently reduced to conidiogenous cells (Fig. 6c, d). Conidiogenous cells are dispersed on hyphae, monoblastic, determinate, variable in shape, mostly subspherical to oblate, hyaline, and 4.8–12.6×6.9–10.5 (mean±SD = 8.8±0.31×8±0.16, n = 30) in size. Conidia are solitary, aseptate, and subglobose to ellipsoidal 10.5–15.6×7.8–13 (mean±SD = 12.8±0.23×10.2±0.2, n = 30; Fig. 6c, d). No

chlamydospores were observed in this study. Sexual morphs were not observed. The size of conidia of this strain closely matched the original description of *N. chinensis* (CGMCC 3.18127)[14]: 10–14.5 × 7.5–11 (mean±SD = 11.78 ± 0.75 × 9.18 ± 0.61) μm.

N. lacticolonia: Isolate no. TAP24N011: Culture characteristics: Colonies on PDA reached 90 mm in diameter. After 3 days of incubation at 25 ± 0.5 °C, the colonies had smooth margins, and were white to whitish gray with abundant cottony aerial mycelia; the reverse was whitish cream to pale brown (Fig. 7a, b). Asexual morph on SNA: Hyphae are hyaline to pale brown, highly-branched, septate, smooth or verrucose, and 2–5.8 (mean±SD = 3.7±0.16, n = 30) μm wide. Conidiophores are micronematous or semi-macronematous, flexuous, hyaline, smooth or verrucose, frequently reduced to conidiogenous cells. Conidiogenous cells are dispersed on hyphae, monoblastic, determinate, variable in shape, mostly subspherical to oblate, hyaline, and 4.6–14.4×5.7–10.9 (mean±SD = 8.2±0.35×7.8±0.2, n = 30) in size (Fig. 7c, d). Conidia are solitary, aseptate, subglobose to ellipsoidal 13.2–16.5×12.2–16.1 (mean±SD = 15.3±0.17×14.9±0.15, n = 30; Fig 7c, d). No chlamydospores were observed in this study. Sexual morphs were not observed. The size of conidia of this strain closely matched the original description of *N. lacticolonia* (CGMCC 3.18123) [14]: 11.5–16.5 (mean±SD. = 14.36 ± 1.04) μm diameter.

Nigrospora sphaerica: Isolate no. TAP24N107: Culture characteristics: Colonies on PDA reached 90 mm in diameter. After 3 days of incubation at 25 ± 0.5 °C, the colonies had smooth margins, and were white to whitish gray with abundant cottony aerial mycelia; the reverse was whitish cream (Fig. 8a, b). Asexual morph on SNA: Hyphae are hyaline to pale brown, branched, septate, smooth, and 1.9–4.2 (mean±SD = 3.1±0.12, n = 30) μm size. Conidiophores are micronematous or semi-macronematous, flexuous, hyaline, smooth, and frequently reduced to conidiogenous cells. Conidiogenous cells are dispersed on hyphae, monoblastic, determinate, variable in shape, mostly subspherical to oblate, hyaline to pale brown, and 6.6–11.7×5.8–17.2 (mean±SD = 9.3±0.23×8.7±0.38, n = 30) in size (Fig. 8c, d). Conidia are solitary, aseptate, subglobose to ellipsoidal 15.6–22.6×15.2–22.9 (mean±SD = 19.6±0.33×19.5±0.36, n = 30; Fig. 8c, d). No chlamydospores were observed in this study. Sexual morphs were not observed. The size of conidia of this strain closely matched the description of *N. sphaerica* (LC2840) measured by Wang et al. [14]: 16–21 (mean±SD = 18.22 ± 1.0) μm diameter.

N. vesicularifera: Isolate no. TAP24N023: Culture characteristics: Colonies on PDA reached 90 mm in diameter. After 3 days of incubation at 25 ± 0.5 °C, the colonies had smooth margins, and were white to whitish gray with abundant cottony aerial mycelia; the reverse was whitish cream to brown (Fig. 9a, b). The isolate did not produce conidia. Sexual morphs were not observed.

Haplotype analyses

Haplotype analysis based on the *tef1α* gene sequences was conducted for *N. lacticolonia*, *N. nigrocolonia*, and *N. singularis*, which were obtained as multiple isolates (Fig. 3a, b). *N. lacticolonia* included 118 isolates, and the alignment consisted of 616 sites. This species was divided into four haplotypes, characterized by six variable sites (S) and a nucleotide diversity (Pi) of 0.001586. Among all the isolates, 78 belonged to Hap_1, 38 to Hap_2, and 1 each to Hap_3 and Hap_4. Hap_1 was found at all six collection sites, whereas Hap_2 was found at five collection sites, excluding Patag-Alanib. Hap_3 was isolated solely from Little Panay, and Hap_4 was isolated solely from Panombon.

N. nigrocolonia included 9 isolates, and the alignment consisted of 714 sites. This species was divided into two haplotypes, with three variable sites (S) and a nucleotide diversity (Pi) of 0.001634. Two isolates belonged to Hap_1, and seven to Hap_2. Both haplotypes were isolated from Dabong-dabong and Patag-Alanib cultivars.

N. singularis included 30 isolates, and the alignment consisted of 604 sites. This species was divided into three haplotypes, with three variable sites (S) and a nucleotide diversity (Pi) of 0.001254. Among all isolates, 21 belonged to Hap_1, 4 to Hap_2, and 5 to Hap_3. Hap_1

was found at five of the collection sites, excluding Panombom, whereas Hap_2 was found at Dabong-dabong and Patag-Alanib. Hap_3 was isolated from the panomboms and patag-alanib.

Pathogenicity to leaves

All 160 isolates were tested on wounded and non-wounded banana leaves. The aggressiveness of the tested isolates on wounded leaves differed significantly, with lesion diameters ranging from 2.33 mm to 22.61 mm (Fig. 10; Table 2; Supplementary Figure 5). Based on diameter sizes of the disease spots, aggressiveness was classified as strongly virulent (≧6.6 mm), moderately virulent (≧3 to <6.6 mm), weakly virulent (> 0 to <3 mm), or very weakly virulent (0 mm with brown or yellow discoloration at or around the wound site). Among the 160 isolates investigated, 54 (33.75%) were strongly virulent, 52 (32.5%) moderately virulent, 43 (26.9%) weakly virulent, and 8 (5%) very weakly virulent; 2 (1.25%) isolates were non-pathogenic. No symptoms appeared on non-wounded banana leaves.

These 160 isolates included six *Nigrospora* species: *N. chinensiss*, *N. lacticolonia*, *N.* cf. *singularis*, *N. sphaeric*a, *N. vesicularifera*, and *N. nigrocolonia*. Among them, *N. chinensis*, *N. sphaerica*, and *N. vesicularifera* were each represented by a single isolate, while multiple isolates were available for *N. lacticolonia*, *N.* cf. *singularis*, and *N. nigrocolonia*. The single isolates of *N. chinensis* exhibited weak virulence. *N. sphaerica*, and *N. vesicularifera* exhibited

strong virulence. In contrast, isolates of *N. lacticolonia*, *N.* cf. *singularis*, and *N. nigrocolonia* showed variable levels of aggressiveness. Among the *N. lacticolonia* isolates, 39.8% (47/118 isolates) were classified as strongly virulent, 37.3% (44/118 isolates) as moderately virulent, 18.6 (22/118 isolates) as weakly virulent, 2.5% (3/118 isolates) as very weakly virulent, and 1.7% (2/118 isolates) as non-pathogenic. For *N.* cf. *singularis*, 16.7% (5/30 isolates) were classified as strongly virulent, 20% (6/30 isolates) as moderately virulent, 50% (15/30 isolates) as weakly virulent, and 13.3% (4/30 isolates) as very weakly virulent. For the isolates of *N. nigrocolonia*, 11.1% (1/9 isolates) were classified as strongly virulent, 22.2% (2/9 isolates) as moderately virulent, 55.5% (5/9 isolates) as weakly virulent, and 11.1% (1/9 isolates) as very weakly virulent.

In vitro fungicide sensitivity test

The heat map in Fig. 11 presents the sensitivity of each isolate of *Nigrospora lacticolonia* (118 isolates), *N. singularis* (30 isolates), *N. nigrocolonia* (9 isolates), *N. chinensis*, *N. sphaerica*, and *N. vesicularifera* (1 isolate each) to each fungicide (active ingredient), using the rate of inhibition of mycelial growth as an indicator (Supplemental Table 1).

All the isolates exhibited high sensitivity (100% inhibition rate) to pyrimethanil (AP) and tebuconazole (DMI). Against pyraclostrobin (QoI), one isolate of *N. lacticolonia* and one isolate

of *N. nigrospora* showed less than 100% sensitivity (72.7% and 92.3%, respectively). Twenty-one isolates were less than 100% (78.7-96.7%) sensitive to chlorothalonil, and 30 isolates less than 100% (74.4-88.5%) sensitive to chlorothalonil. Both fungicides resulted in 100% inhibition of the remaining isolates. Seventy-seven isolates of *N. lacticolonia* exhibited less than 100% (70.1-86.6%) sensitivity to boscalid (SDHI). One isolate (76.9%) of *N. singularis* and one isolate (84.7%) of *N. nigrocolonia* exhibited less than 100% sensitivity. Sixty-nine isolates of *N. lacticolonia* exhibited a range of 79.9–98% sensitivity to fluxapyroxad. One isolate (80.6%) of *N. singularis* and two (83.2-85.8%) of *N. nigrocolonia* had less than 100% sensitivity. Twenty-two isolates of *N. lacticolonia* displayed sensitivities ranging from 88.8–98.1% to fluopyram. One isolate (67.9%) of *N. nigrocolonia* exhibited less than 100% sensitivity. All isolates were highly sensitive to the GMI agents bitertanol, difenoconazole, and epoxiconazole, except for one to two isolates of *N. nigrocolonia* (72-94.8% inhibition rate). With the exception of nine isolates of *N. singularis* and one isolate each of *N. sphaerica* and *N. vesicularifera*, the inhibition rates of fenpropimorph (SBI class 2) were less than 100% (16.9-90.7%). In contrast, all fungi were highly sensitive (100%) to spiroxamine, which belongs to the same class as fenpropimorph.

The dominant species, *N. lacticolonia*, exhibited low sensitivity to 8 of the 14 fungicides. The second most dominant species, *N. singularis*, presented low sensitivity to the four species.

N. nigrocolonia exhibited low sensitivity to nine fungicides, while *N. chinensis* and *N. vesicularifera* exhibited low sensitivity to one.

Principal component analysis (PCA) for fungicide sensitivety

PCA was performed based on inhibition rates (Supplemental Table 1). In the final PCA results, data for TAP24N093, TAP24N094, TAP24N163, and TAP24N252, which appeared as outliers, were excluded (Supplementary Figure 6). These outliers were determined based on principal component scores obtained from PCA, using a threshold of three standard deviations from the mean for PC1 and PC2. This criterion is grounded in the statistical property of the normal distribution, where approximately 99.7% of data points fall within ±3 standard deviations. PC1 and PC2 together explained 37.99% of the total variance in the dataset (Supplementary Figure 7; Supplementary Table 2). For PC1, the top three contributors were Chlorothalonil (22.7%), Mancozeb (21.6%), and Fluopyram (16.5%). For PC2, the top three contributors included Flutriafol (53.8%), Fluxapyroxad (18.8%), and Difenoconazole (14.8%). Cluster analysis, based on the distances between the coordinates in the two-dimensional scatter plot of PC1 and PC2, revealed that no distinct clusters were formed within the specific regions or fungal lineages (Fig. 12). In cases where PCA was performed including the four strains

identified as outliers, no clustering by geographic region or haplotype was observed, consistent with the results obtained after excluding the outliers (Supplementary Figure 8).

Discussion

This study aimed to provide essential information for managing leaf spot diseases in the Philippines. To this end, we identified pathogens responsible for banana leaf diseases in Mindanao, the main banana-producing region in the Philippines, and evaluated the efficacy of 14 fungicides currently in use against these pathogens.

On Mindanao Island, the disease "black Sigatoka," caused by *Pseudocercospora fijiensis*, was suspected but not detected in any of the sampled locations. Eighteen genera of fungi from symptomatic leaves were collected from six farms in Mindanao, and the most prevalent genus was *Nigrospora* spp., accounting for 72% of the total fungal isolates.

The isolated isolates were identified as six species: *N. chinensis*, *N. lacticolonia*, *N. nigrocolonia*, *N. singularis*, *N. sphaerica*, and *N. vesicularifera*, all of which are pathogens that infect banana leaves. To the best of our knowledge, this is the first report of *N. chinensis*, *N. lacticolonia*, *N. nigrocolonia*, *N. singularis*, and *N. vesicularifera* as causative agents of banana leaf spot worldwide. *N. sphaerica* has previously been reported as the causal agent of banana “leaf spot” in Bangladesh[7], but this is the first report of *N. sphaerica* in the Philippines.

In the Philippines, chemical spraying is a common agricultural practice employed 50–70 times per year to manage the local incidence of Sigatoka disease. Frequent use of fungicides may have altered the leaf biota community and created a selective pressure that allowed for the persistence of resistant species or strains. However, this cross-sectional study cannot establish causality. *Pseudocercosporaceae* fungi are inherently slow-growing; therefore, during this study, they may have been overgrown by other co-infecting fungi and remained undetected. Therefore, the presence of *P. fijiensis* at the survey sites is not discussed in this study. Nevertheless, it should be hypothesized that *P. fijiensis* may have been subjected to selection pressure from fungicide application, potentially contributing to the emergence of the genus *Nigrospora* as the dominant pathogen at the sampling sites. Future verification through pathogen-specific PCR detection on infected leaves is considered necessary.

An example of consequence fungicide application contributing to changes in the fungal composition of pathogenic communities has been reported in wheat [15]. This raises concerns regarding the selection of fungicides, as they may lead to a shift in the pathogenic fungi present on banana leaves. To ensure the continued efficacy of fungicide applications in banana cultivation, conducting regular surveys on disease incidence and fungicide sensitivity, specifically targeting *Nigrospora* and *Pseudocercospora* species, is essential.

Among the 160 isolates of the six species of the genus *Nigrospora*, *N. lacticolonia* accounted for 74% of the total (118 isolates). This species was identified as the dominant species at four sites: Little Panay, Panambong, Tugbok, and Ula. Conversely, *N. singularis* was dominant in Patag-Alanib and Dabong-dabong. The isolation frequencies of *N. nigrocolonia*, *N. sphaerica*, and *N. vesicularifera* were comparatively lower than those of the two species, and they are not currently considered primary pathogens of banana leaf spot.

Haplotype analysis revealed that *N. lacticolonia* Hap_1 and Hap_2 were detected in all six regions and five regions, respectively, while *N. singularis* Hap_1 was detected in five regions. The observation that the same haplotype was detected in multiple regions suggests that genetically similar populations are widely distributed across Mindanao Island, indicating past population migration and diffusion.

Furthermore, a comprehensive analysis of the sensitivity to 14 chemical substances using principal component analysis (PCA) revealed that the distribution of PCA on the graph did not reflect the classification of fungal species or haplotypes. Isolates exhibiting different sensitivities to 11 chemicals (excluding tebuconazole, spiroxamine, and pyrimethanil) were found within the species and haplotypes. Notably, the distribution of the isolates did not align with the classification of species or haplotypes. This indicates that fungicide sensitivity among the isolates may have evolved independently of species or haplotype differentiation. This

hypothesis is further supported by the findings of Hartmann et al. [16], who demonstrated that mutations in CYP51, linked to azole fungicide resistance, and Cytb, associated with strobilurine (QoI) resistance, emerged independently in distinct geographical regions. Therefore, this observation suggests that the fungicide sensitivity in the isolates arose independently of species and haplotype differentiation. However, because this study did not include a genetic analysis of fungicide resistance, the ensuing discussion focuses on the potential mechanisms underlying the acquisition of fungicide resistance. Hartmann et al. [16] noted that gene flow resulting from human migration and spore dispersal contributes to the ectopic occurrence of resistant isolates. The dispersal of diseases caused by *Nigropsora* spp. on Mindanao Island is not only attributable to human migration resulting from the movement of soil and seedlings but also to soil runoff caused by flooding and atmospheric migration. The potential contribution of soil runoff is supported by the detection of this genus in both soil [17] and atmospheric environments [15]. Consequently, it can be posited that fungi with acquired resistance have a propensity for dissemination.

Therefore, elucidating the mechanisms underlying the dissemination of pathogenic fungi is imperative for effective disease control. This includes controlling resistant isolates and determining the optimal timing for disinfectant application. Meredith [18] demonstrated that the spores of *Nigrospora* spp. are released into the atmosphere in a diurnal cycle. Specifically, in

Jamaica, spore release commenced at approximately 7:00 a.m., reaching a peak between 8:00 and 10:00 a.m. This diurnal pattern suggests that *Nigrospora* spp. employ a release mechanism that functions under decreasing vapor pressure [19], which is crucial information for disease control. However, further research is necessary to investigate the environmental factors associated with disease outbreaks in banana plantations in the Philippines.

The findings of this study regarding pathogen sensitivity to fungicides are fundamental data. However, as this is an urgent issue, it is important to note that all 118 isolates of *N. lacticolonia*, the most frequently isolated fungus species, exhibited moderate or low sensitivity to fenpropimorph (inhibition rate 16.9–90.7%). The fungicide is unlikely to be effective because the low in vitro sensitivity suggests that its inhibitory capabilities in the field will likely remain low. In contrast, all fungi showed high sensitivity to spiroxamine, a fungicide of the same class (SBI classification II group), with 100% inhibition of mycelial growth. Notably, the use of these fungicides raises concerns regarding potential cross-resistance, and it is possible that fungi resistant to spiroxamine may emerge in the future. Based on these results, we propose that the emergence of cross-resistant fungi should be monitored.

In this study, we showed that banana leaf diseases occurring in Mindanao are not black Sigatoka caused by *P. fijiensis* but are mainly leaf blight caused by six species belonging to the genus *Nigrospora*. As important information for disease control, it was considered that fungal

senescence may occur due to fungicide treatments, as some of these are sensitive to the 14 fungicides used for black Sigatoka disease, while others are not. It is recommended that further surveys of fungal diseases throughout Mindanao Island be conducted and that fungicide selection for disease control be based on a comprehensive understanding of banana leaf diseases.

Materials and methods

Isolation of fungi

In July 2024, 175 of banana leaves (27 to 30 leaves from each banana plantation) with Sigatoka-like symptoms were collected at 6 Cavendish banana plantations located in “Barangay Dabong-dabong, Valencia City, Bukidnon (7°58′28″N 125°4′55″E; altitude: 313 m)” (29 leaves), “Barangay Little Panay, Panabo, Davao del Norte (7°17′44″N 125°38′46″E; altitude: 17 m)” (30 leaves), “Barangay Panombon, Mati, Davao Oriental (7°0′32″N 126°16′28″E; altitude: 20 m)” (30 leaves), “Barangay Patag-Alanib, Lantapan, Bukidnon (8°1′5″N 125°1′57″E; altitude: 851 m)” (27 leaves), “Barangay Tugbok, Davao City, Davao del Sur (7°11′45″N 125°27′23″E; altitude: 217 m)” (29 leaves), and “Barangay Ula, Davao City, Davao del Sur (7°8′16″N 125°29′37″E; altitude: 291 m) (30 leaves)” in Mindanao Island, Philippines (Fig. 13). Banana plants selected for sampling were estimated to be between five and eight months of age. Symptoms included small spots with gray centers and yellow halos, as well as spots that turned

brown or dark brown as they expanded. The leaves also showed signs of coalescing lesions as the spots expanded. Fungi were isolated from the symptoms, including black and brown spots and yellow hallows (Fig. 7). Plant tissues with apparent symptoms were cut into 3-mm square segments, sterilized with 0.6% (v/v) sodium hypochlorite for 1 min, rinsed twice with sterilized water, and placed on water agar plates. To obtain monocultures of fungal isolates, a single hypha was picked directly from the mycelium that emerged from the tissues on water agar. Colonies with different appearances in a single sample were individually isolated, and then transplanted onto potato dextrose agar (PDA) plates. The monoculture isolates were deposited in the culture collection at Tamagawa University and maintained on PDA plates.

Polymerase chain reaction (PCR)

Template DNA for PCR was obtained from the mycelia of each isolate grown on potato dextrose agar for 7 d using a CTAB method [20]. PCR was performed using a 10 μL PCR mixture containing 7 μL distilled water, 1 μL 10× Ex Taq buffer with $MgCl_2$, 0.8 μL dNTP (10 mM each), 0.1 μL of each primer (50 μM), 0.05 μL Ex Taq DNA polymerase (5 U μL^{-1}, Takara, Tokyo, Japan), and 1.0 μL of DNA template. For DNA sequencing of all 160 isolates, the partial 18S rRNA gene, ITS1, 5.8S rRNA gene, ITS2, and partial 28S rRNA gene internal transcribed spacer (ITS) regions were amplified using primer pairs ITS4 and ITS5 [21]. For 107 isolates of *Nigrospora* fungi, in addition to the ITS region, two DNA regions, partial sequences of the *β*-

tubulin and the *transcribed elongation factor 1 alfa* (*tef1*) genes, were amplified by using primer pairs Bt2a and Bt2b [22] and Nigro_EF1 (5'-AAC ATC GTC GTT ATC GGC CA-3') and Nigro_EF2 (5'-TGA TCT CCT TGT AAC GGG CC-3') (designed in this study), respectively. As the commonly used primers EF1 and EF2 failed to amplify the tef1 region from the isolates obtained in this study, Nigro_EF1 and Nigro_EF2 was newly designed in this study (Supplementary Figure 9).

The PCR was performed under the conditions listed in Table 3. PCR reaction primers were used for sequencing. PCR products were sequenced by the FASMAC Co. Ltd. in Japan (https://fasmac.co.jp/). Obtained forward and reverse sequence reads were assembled using BioEdit v7.7.1.0 software [23] (https://thalljiscience.github.io/page2.html).

Molecular phylogenetic analysis

To identify the 217 isolates at the genus level, we used ITS region sequences to conduct a BLAST search in the NCBI database. Based on the results of the BLAST search, we selected 160 isolates belonging to the genus *Nigrospora* for further analyses to determine the dominant species and diversity of pathogens in the genus *Nigrospora*. To construct phylogenetic trees, 160 isolates and 36 strains of *Nigrospora* spp., including ex-type strains, were used as ingroup taxa (Table 4). As an out group, *Apiospora malaysiana* and *A. pseudoparenchymatica* were selected

from the genus *Apiospora*, which is a sister group to the genus *Nigrospora*. All of the ITS, *β-tubulin*, and *tef1* sequences were used for multiple alignments by ClustalW with BioEdit [23] and concatenated into one dataset (Supplementary data 1). Bayesian Inferences (BI) with MrBayes 3.1.2 [24] (https://nbisweden.github.io/MrBayes/index.html) implementing the Markov chain Monto Carlo technique were performed based on the combined dataset of ITS, *β-tubulin*, and *tef1α*. The best-fitted model for each locus for BI was selected with MrMODELTEST2.3 [25]. Each locus was treated as a separate partition. The parameters in MrBayes were set as follows: lset nst = 6, 2, and 6 for ITS, β-tubulin, and *tef1α*, respectively; rates = invgamma, prset statefreqpr = dirichlet (1,1,1,1), nchains = 4, temp = 0.2, swapfreq = 1, and nswaps = 1. The Markov chains were continued until average standard deviation of split frequencies fell below 0.0095 (7,305,000 generations). Only trees sampled after the average standard deviation of split frequencies dropped below 0.01 were used for consensus tree construction. Accordingly, the first 7,244,000 generations were discarded as burn-in. The remaining trees were used to construct a 50% majority-rule consensus tree. Branches that received Bayesian posterior probabilities (BPP) greater than or equal to 0.95 were considered as significantly supported. Bayesian analysis was also performed for each locus with the model described above, and using same parameters. For BI based on ITS and *β-tubulin* sequences, the Markov chains were continued until average standard deviation of split frequencies fell below

0.0095 (27,815,000 and 1,835,000 generations, respectively). Only trees sampled after the average standard deviation of split frequencies dropped below 0.01 were used for consensus tree construction. Accordingly, the first 28,761,000 for ITS and 1,760,000 for *β-tubulin* generations were discarded as burn-in. For BI based on *tef1α*, despite running the analysis for 40,000,000 generations, the average standard deviation of split frequencies did not fall below 0.01. Therefore, we constructed the phylogenetic tree using 1,000 generations of data starting from generation 28,761,000, which yielded the lowest average standard deviation of split frequencies value (0.016862).

Phylogenetic analyses with maximum likelihood method were performed using Molecular Evolutionary Genetics Analysis (MEGA10) software (Kumar 2018) [26]. Tamura-Nei model was selected as the best substitution model based on the Akaike information criterion using MEGA 10. All sites with gaps were treated as missing data. The reliability of each internal branch in the phylogenetic trees was assessed using bootstrap analysis with 1,000 random-addition replicates [27].

Morphological observation

Our isolates were cultured on synthetic low-nutrient agar (SNA) [28] at 28□ for 10 days to induce sporulation in the dark. The shape and size of the microscopic structures were observed using light microscopy (B51, Olympus, Tokyo, Japan), and the colonies were assessed. At least

30 conidiogenous cells and conidia were measured to determine mean colony size. Three SNA plates were examined, and from each plate, ten or more conidiophores and conidia were observed for measurement. These measurements were conducted using ImageJ 1.52a software (Rasband, WS, ImageJ; US National Institutes of Health: https://imagej.net/ij/index.html).

Pathogenicity test

Each of our 160 isolates was tested for pathogenicity using mycelial discs (5 mm diameter) obtained from the edges of colonies grown on PDA media for three days. These discs were then applied to four sites on non-wounded and wounded segments of healthy banana leaves (approx. 5×5 cm in size; cv. Dwarf Cavendish). For each fungal strain, two non-wounded and two wounded leaf segments were used. Three puncture sites were created on the wounded leaves using a heated sewing needle. Each puncture site was spaced approximately 2 mm apart. The inoculated leaves were covered with plastic boxes to maintain high humidity (85–90%) with wet paper towel and maintained at approximately 25 °C under natural light condition for three days. PDA was used as a control. Pathogenicity was evaluated based on the size and coloration of lesions observed at 4 days after inoculation (dpi). Isolates that did not produce elliptical necrotic lesions but caused brown or yellow discoloration at or around the wound site were considered extremely weak in pathogenicity and were classified as “very weakly virulent”. For isolates that formed brown, spindle-shaped necrotic lesions, the lesion length at each of the eight inoculation

points was measured, and the mean lesion length was used as an index of pathogenicity. To further categorize the degree of pathogenicity, the 33rd and 66th percentiles of the mean lesion lengths were calculated. Isolates with mean values below the 33rd percentile were classified as "weakly virulent", those between the 33rd and 66th percentiles as "moderate virulent", and those above the 66th percentile as "strongly virulent". This classification was performed using R (version 4.2.2), with data processing conducted via the dplyr package. Values of zero were excluded prior to quantile calculation. Based on these criteria, all isolates were ultimately categorized into five levels of pathogenicity: "non-pathogenic", "very weakly virulent", "weakly virulent", "moderate virulent", and "strongly virulent". At 7 dpi, the symptoms appeared, the fungi were re-isolated from the diseased tissue using the same method as that of the description in "isolation of fungi" and re-identified based on morphologies of colony on PDA.

Haplotype analyses

The haplotypes of *N. lacticolonia*, *N. singuralis*, and *N. nigrocolonia* were analyzed to reveal the spread of pathogens on Mindanao Island. The sequence of the *tef1α* gene was used for the analyses because mutations in each species were observed in the gene. The *tef1α* gene sequences for each species were aligned using MEGA 10, and sites containing gaps at both ends were trimmed. The total number of variable sites (S) and the nucleotide diversity (Pi) were

calculated using MEGA 10. The trimmed alignment data were exported to PopArt v1.7 [29] to construct a haplotype network. The geographic distribution of the haplotypes was visualized using the median-joining option in the PopArt program.

In vitro Fungicide Sensitivity test

In vitro tests were conducted to evaluate the inhibitory effects of the active ingredients in fungicides, currently used in the Philippines, on the mycelial growth of *Nigrospora* spp. Mycelial growth inhibition was used as an indicator of sensitivity. The active ingredients of 14 fungicides belonging to 6 classes of the Fungicide Resistance Action Committee (FRAC) were dissolved in acetone or sterile distilled water and adjusted to a concentration of 1/5 in PDA medium. Aryl hydroxamic acid (SHAM; Fluorochem Ltd.) was used in conjunction with the QoI fungicide pyraclostrobin to inhibit alternative oxidase (AOX), which does not react with cyano groups [30,31]. The final concentrations of the fungicides in the medium were as follows: 100 ppm for bitertanol, difenoconazole, epoxiconazole, flutriafol, tebuconazole, fenpropimorph, spiroxamine, boscalid, and flusapirox; and 200 ppm for mancozeb and chlorothalonil. Media without fungicides (0 ppm) were used as control to formulate inhibition rate. These fungicide concentrations were determined based on the following reasons. In FRAC monitoring assays, the upper concentration range typically falls between 1 and 30 ppm; however, concentrations as high as 100 ppm are occasionally employed. By intentionally setting the concentration higher

than the standard FRAC monitoring range, we aimed to detect isolates with clearly low sensitivity. Isolates were classified as sensitive or low-sensitive based on their growth response at 100 ppm or 200 ppm. Those exhibiting visible growth at these concentrations were designated as having low sensitivity.

Mycelial disks (6 mm in diameter) were obtained from the periphery of pre-cultured colonies, which were cultured at 25°C for 3 days in 1/5 PDA. These disks were transferred to 1/5 PDA containing the chemicals at avobe mentioned concentrations. Following a 24-h incubation period at 25°C, the diameters of the colonies were measured, and 6 mm was subtracted from the diameter of the mycelial disc. The inhibition rate was defined as the rate of growth when the control was 100%, and was calculated from the values of the four colonies.

Principal component analysis (PCA)

The PCA of standardized variables was performed using R (v4.2.2) to determine whether there was a difference in the inhibition rate among species/haplotypes and sampling sites. We conducted PCA using the inhibition rate data obtained from the 14 fungicides as variants. The final principal components (PCs) were determined by excluding the data of individuals that fell outside the ±3σ range as outliers. Euclidean distances were calculated based on the obtained coordinates of PC1 and PC2, and a dendrogram was constructed using Ward's method. Outliers were defined based on principal component scores obtained from PCA, using a threshold of

three standard deviations from the mean for PC1 and PC2. This criterion is grounded in the statistical property of the normal distribution, where approximately 99.7% of data points fall within ±3 standard deviations. Values exceeding this range are considered statistically rare and thus indicative of potential outliers. A sample was classified as an outlier if either its PC1 or PC2 score exceeded the threshold.

Acknowledgments

We are grateful to Ms Sayuri Sakurai (Tamagawa University BacaDM Project) for her assistance in preparing the culture medium for this research.

Data Availability

The datasets generated during the current study are available in the GenBank provided by NCBI/DDBJ. The GenBank accession numbers are listed in Table 4.

Author Contribution

S.N. conceived the study, designed the methodology, collected field samples, conducted fungicide sensitivity tests, conducted all analyses, visualization of the data, and led the manuscript preparation. Y.H. and Y.T. conducted fungicide sensitivity tests. K.U. designed the methodology for fungicide sensitivity tests. M.A.M., R.V., S.M.C., and A.F.P. collected field samples. K.W. supervised this study, acquired funding, conducted fungicide sensitivity tests, and

assisted in manuscript editing and project coordination. All authors reviewed and approved the final manuscript

Competing Interests Statement

The authors declare no competing interests.

References

1. Nozawa, S. et al. *Fusarium mindanaoense* sp. nov., a new fusarium wilt pathogen of cavendish banana from the Philippines belonging to the F. fujikuroi species complex. *J. Fungi (Basel)* **9**, 443; 10.3390/jof9040443, PubMed: 37108898 (2023).
2. Ploetz, R. C. Fusarium wilt of banana. *Phytopathology* **105**, 1512–1521; 10.1094/PHYTO-04-15-0101-RVW, PubMed: 26057187 (2015).
3. Wang, B. et al. A new leaf blight disease caused by *Alternaria jacinthicola* on banana in China. *Horticulturae* **8**, 12 (2021).
4. Fu, B. Z. et al. First report of leaf spot caused by *Alternaria alternata* on Chinese dwarf banana in China. *Plant Dis.* **98**, 691-691; 10.1094/PDIS-08-13-0831-PDN, PubMed: 30708541 (2014).
5. Huang, R. et al. Identification and characterization of Colletotrichum species associated with anthracnose disease of banana. *Plant Pathol.* **70**, 1827-1837; 10.1111/ppa.13426 (2021).

6. Crous, P. W. & Mourichon, X. Mycosphaerella eumusae and its anamorph *Pseudocercospora eumusae* spp. nov: causal agent of eumusae leaf spot disease of banana. *Sydowia* **54**, 23-34 (2002).

7. Sadid, K. N. E., Hossain, M. A., Munshi, A. R. & Karim, M. R. First detection, isolation and molecular characterization of banana leaf spot diseases caused by *Nigrospora sphaerica* and *Neocordana musae* in Bangladesh. *Arch. Phytopathol. Plant Prot.* **56**, 1112-1125 (2023).

8. Fortune, M. P. et al. First report of black Sigatoka disease (causal agent *Mycosphaerella fijiensis*) from Trinidad. *Plant Pathol.* **54**, 246; 10.1111/j.1365-3059.2005.01123.x (2005).

9. Strobl, E. & Mohan, P. Climate and the global spread and impact of bananas' black leaf sigatoka disease. *Atmosphere* **11**, 947; 10.3390/atmos11090947 (2020).

10. Esguera, J. G., Balendres, M. A. & Paguntalan, D. P. Overview of the Sigatoka leaf spot complex in banana and its current management. *Trop. Plant* **3**, e002; 10.48130/tp-0024-0001 (2024).

11. Rhodes, P. L. A new banana disease in Fiji. *CPN* **10**, 38–41 (1964).

12. Pordel, A., Dehghani, K., Amirmijani, A. & Miri, K. Identification and pathogenicity of Fusarium sensu lato species causeing wilting and leaf spot of Banana in South of Iran. *Iran. J. Plant Pathol.* **58**, 96-108 (2022).

13. Raza, M. et al. Culturable plant pathogenic fungi associated with sugarcane in southern China. *Fungal Divers*. **99**, 1–104; 10.1007/s13225-019-00434-5 (2019).

14. Wang, M et al. Phylogenetic reassessment of *Nigrospora*: Ubiquitous endophytes, plant and human pathogens. *Persoonia* **39**, 118–142; 10.3767/persoonia.2017.39.06 (2017).

15. Karlsson, I., Friberg, H., Steinberg, C. & Persson, P. Fungicide effects on fungal community composition in the wheat phyllosphere. *PLOS One* **9**, e111786; 10.1371/journal.pone.0111786, PubMed: 25369054 (2014).

16. Hartmann, F. E. et al. The complex genomic basis of rapid convergent adaptation to pesticides across continents in a fungal plant pathogen. *Mol. Ecol.* **30**, 5390-5405; 10.1111/mec.15737, PubMed: 33211369 (2021).

17. Zhang, Y. Y. et al. *Nigrospora humicola* (Apiosporaceae, Amphisphaeriales), a new fungus from soil in China. *Diversity* **16**, 118 (2024).

18. Meredith, D. S. Atmospheric content of nigrospora spores in Jamaican banana plantations. *J. Gen. Microbiol.* **26**, 343-349; 10.1099/00221287-26-2-343, PubMed: 14472772 (1961).

19. Hirst, J. M. Changes in atmospheric spore content: diurnal periodicity and the effects of weather. *Trans Br Mycol Soc.* **36**, 375–IN8; 10.1016/S0007-1536(53)80034-3 (1953).

20. Doyle, J. J. & Doyle, J. L. A rapid DNA isolation procedure for small quantities of fresh leaf tissue. *Phytochem Bull.* 19A1 **A27**, 11–15 (1987).

21. White, T. J., Bruns, T., Lee, S. & Taylor, J. W. Amplification and direct sequencing of fungal ribosomal RNA genes for phylogenetics. in 15 (ed. Gelfand, D. H., Shinsky, J. J. & White, T. J.) PCR Protocols: A Guide to Methods and Applications Ch. 315–322 (M.A., Innis) (Acad. Press (San Diego, 1990)).

22. Glass, N. L. & Donaldson, G. C. Development of primer sets designed for use with the PCR to amplify conserved genes from filamentous Ascomycetes. *Appl Environ Microbiol.* **61**, 1323-1330; 10.1128/aem.61.4.1323-1330.1995, PubMed: 7747954 (1995).

23. Hall, T. A. BioEdit: a user-friendly biological sequence alignment editor and analysis program. for Windows 95/98/NT. *Nucleic Acids Symp Ser.* 41 95–98, (1999).

24. Ronquist, F. & Huelsenbeck, J. P. MrBayes 3: Bayesian phylogenetic inference under mixed models. *Bioinformatics* **19**, 1572–1574 (2003).

25. Nylander, J.A. Modeltest v2. Program distributed by the author. Evolutionary Biology Centre, Uppsala University (2004).

26. Kumar, S., Stecher, G., Li, M., Knyaz, C., Tamura, K. et al. MEGA X: Molecular evolutionary genetics analysis across computing platforms. *Mol. Biol. Evol.* **35**, 1547–1549; 10.1093/molbev/msy096, PubMed: 29722887 (2018).

27. Felsenstein, J. Confidence limits on phylogenies: an approach using the bootstrap. *Evolution* **39**, 783–791; 10.1111/j.1558-5646.1985.tb00420.x, PubMed: 28561359 (1985).

28. Nirenberg, H. I. A simplified method for identifying Fusarium spp. occurring on wheat. *Can. J. Bot.* **59**, 1599–1609 (1981).

29. Leigh, J. W. & Bryant, D. POPART: full-feature software for haplotype networkconstruction. *Methods Ecol. Evol.* **6**, 1110-1116; 10.1111/2041-210X.12410 (2015).

30. Ishii, H. et al. Characterisation of QoI resistant field isolates of Botrytis cinerea from citrus and strawberry. *Pest Manag. Sci.* **65**, 916-922; 10.1002/ps.1773, PubMed: 19444805 (2009).

31. Hollomon, D. W., Wood, P. M., Reeve, C. & Miguez, M. Alternative oxidase and its impact on the activity of Qo and Qi site inhibitors. in *Modern Fungicides and Antifungal Compounds IV* (ed. Dehne, H. W., Gisi, U., Kuck, K. H., Russell, P. E. & Lyr, H.) 31–34 (BCPC, Alton, Hants, UK, 2005).

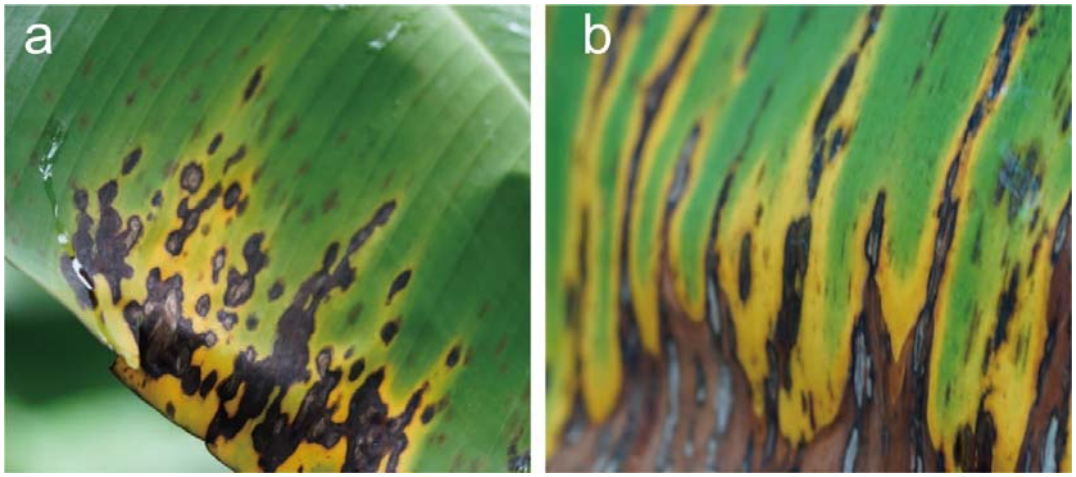

Fig. 1 Symptoms of leaf spot on banana leaves in fields. Naturally infected leaves in banana plantations (a, b).

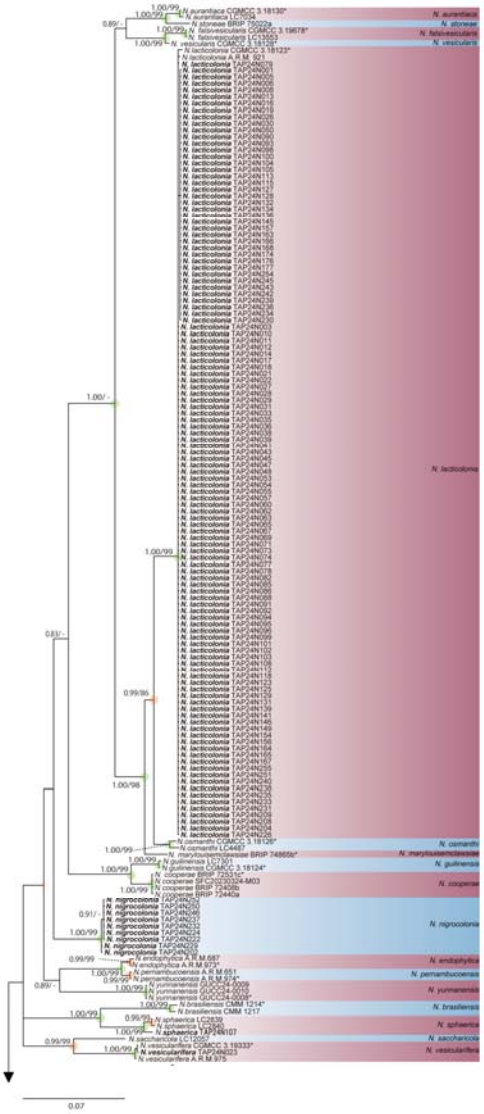

Fig. 2 Phylogenetic trees constructed based on the concatenated data of the DNA sequences of ITS, *β-tubulin*, and *tef1α* genes inferred using MrBayes. HKY, GTR, and HKY was used as models in MrBayes for ITS, *β-tubulin*, and *tef1α*, respectively. The numbers on the left and right of each node are posterior probabilities estimated using the software MrBayes and bootstrap values from ML method performed with MEGA 10 with Tamura-Nei model, respectively. Nodes with a PPB of 1.0 are highlighted with green circles, while those with PPB ≥ 0.95 are indicated by orange circles. Strain number with asterisk is ex-type strain. Species name and strains with boldface is our isolate. Branch lengths are proportional to the number of substitutions per site; the scale bar indicates expected substitutions per site.

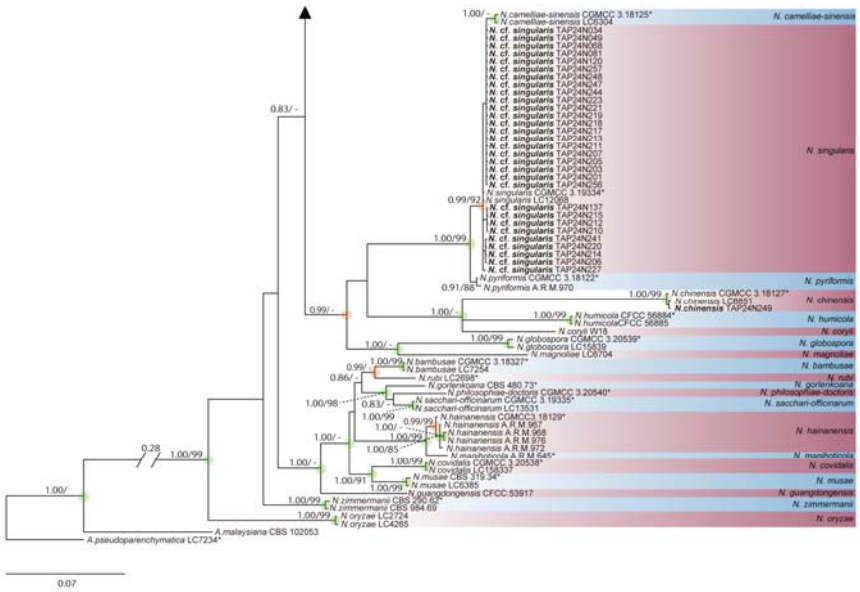

Fig. 2 Continued.

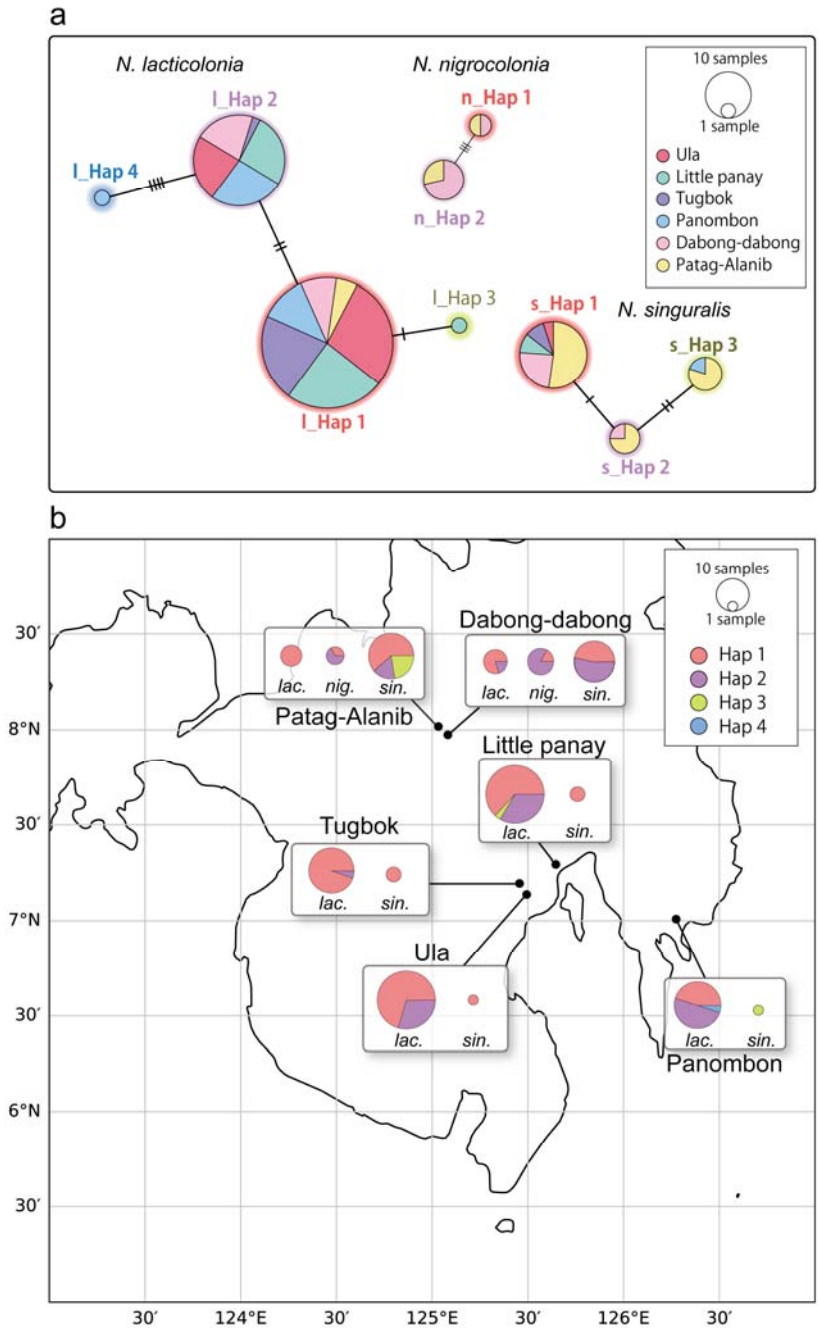

Fig. 3 Haplotype analyses of *N. lacticolonia, N. niglospora,* and *N. singularis*. Haplotype networks (a). l_Hap; *N. lacticolonia* haplotype, n_Hap; *N. nigrospora* haplotype, and s_Hap; *N. singularis* haplotype. Distribution of species and haplotypes in the Mindanao Island, Philippines (b). *lac*; *N. lacticolonia*, *nig*; *N. nigrospora*, and *sin*; *N. singularis.* The size of the circle depends on the number of samples.

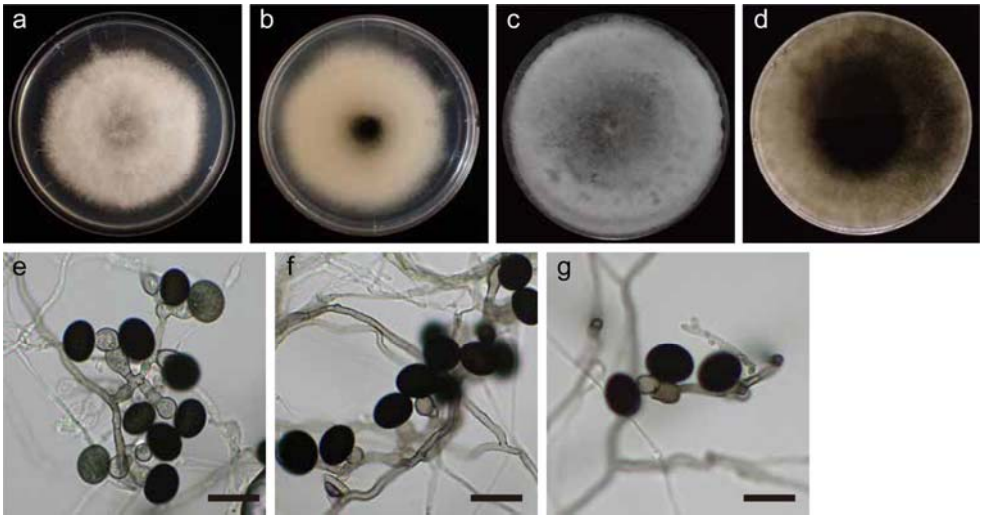

Fig. 4 ***Nigrospora nigrocolonia*** **(TAP24N237).** Surface and reverse of colony on PDA after 3 days (a, b) and 7 days (c, d). Conidiogenous cells and conidia on SNA plate (e, f, g). Scale bars: = 20 μm

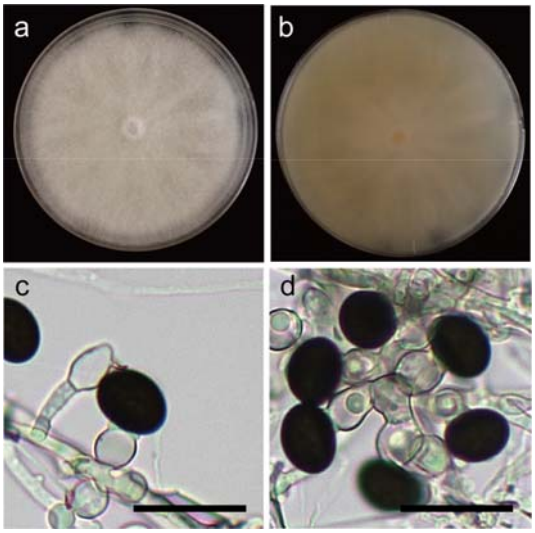

Fig. 5 ***Nigrospora chinensis*** **(TAP24N249).** Surface and reverse of colony on PDA after 3 days (a, b). Conidiogenous cells and conidia on SNA plate (c, d). Scale bars: = 20 μm

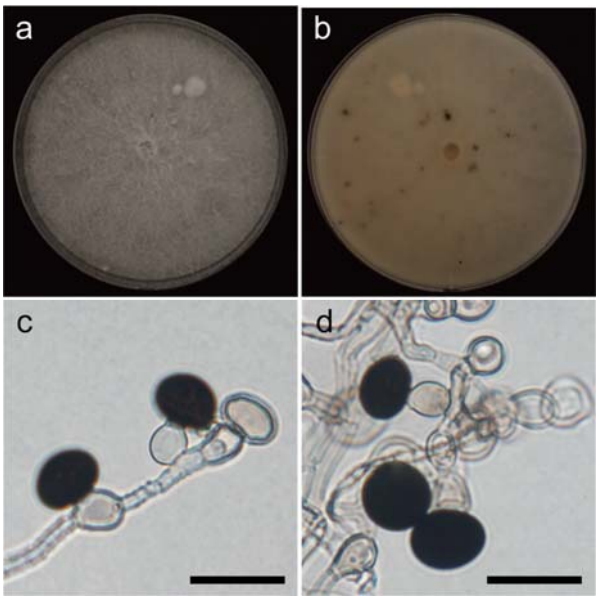

Fig. 6 ***Nigrospora lacticolonia*** **(TAP24N011).** Surface and reverse of colony on PDA after 3 days (a, b). Conidiogenous cells and conidia on SNA plate (c, d). Scale bars: = 20 μm

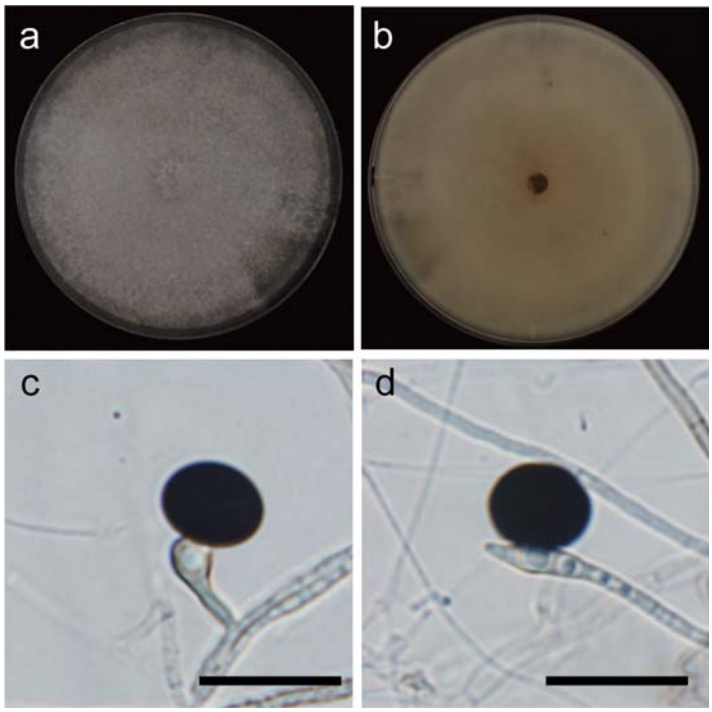

Fig. 7 ***Nigrospora singuralis*** **(TAP24N068).** Surface and reverse of colony on PDA after 3 days (a, b). Conidiogenous cells and conidia on SNA plate (c, d). Scale bars: = 20 μm

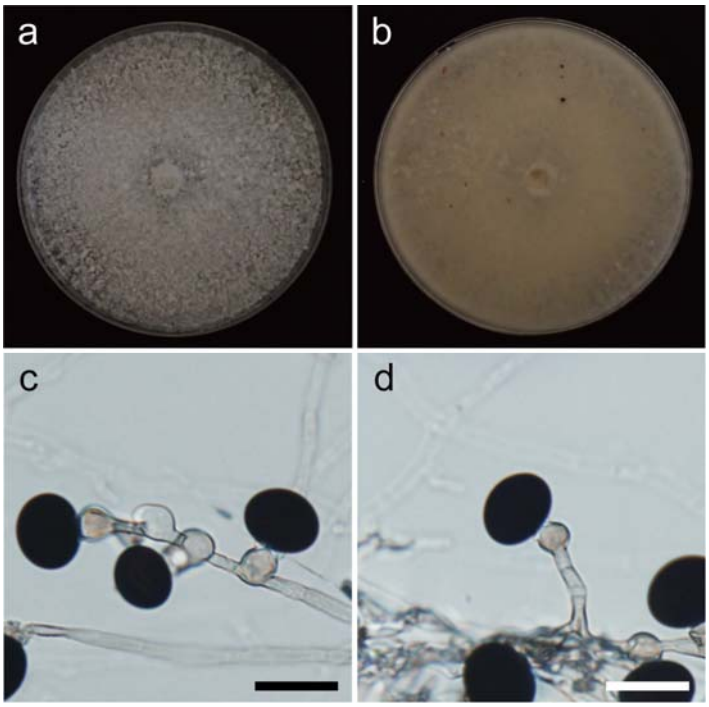

Fig. 8 ***Nigrospora sphaerica*** **(TAP24N107).** Surface and reverse of colony on PDA after 3 days (a, b). Conidiogenous cells and conidia on SNA plate (c, d). Scale bars: = 20 μm

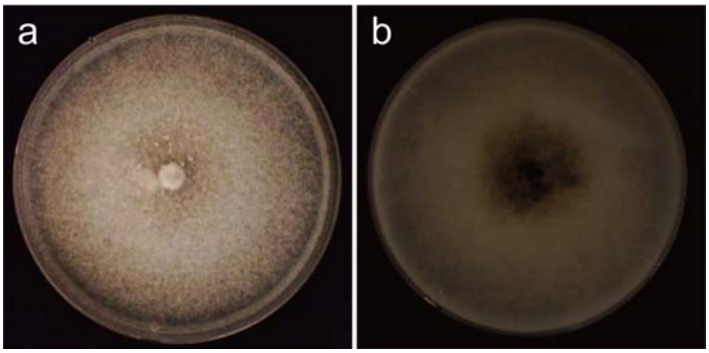

Fig. 9 ***Nigrospora vesicularifera*** **(TAP24N023).** Surface and reverse of colony on PDA after 3 days (a, b).

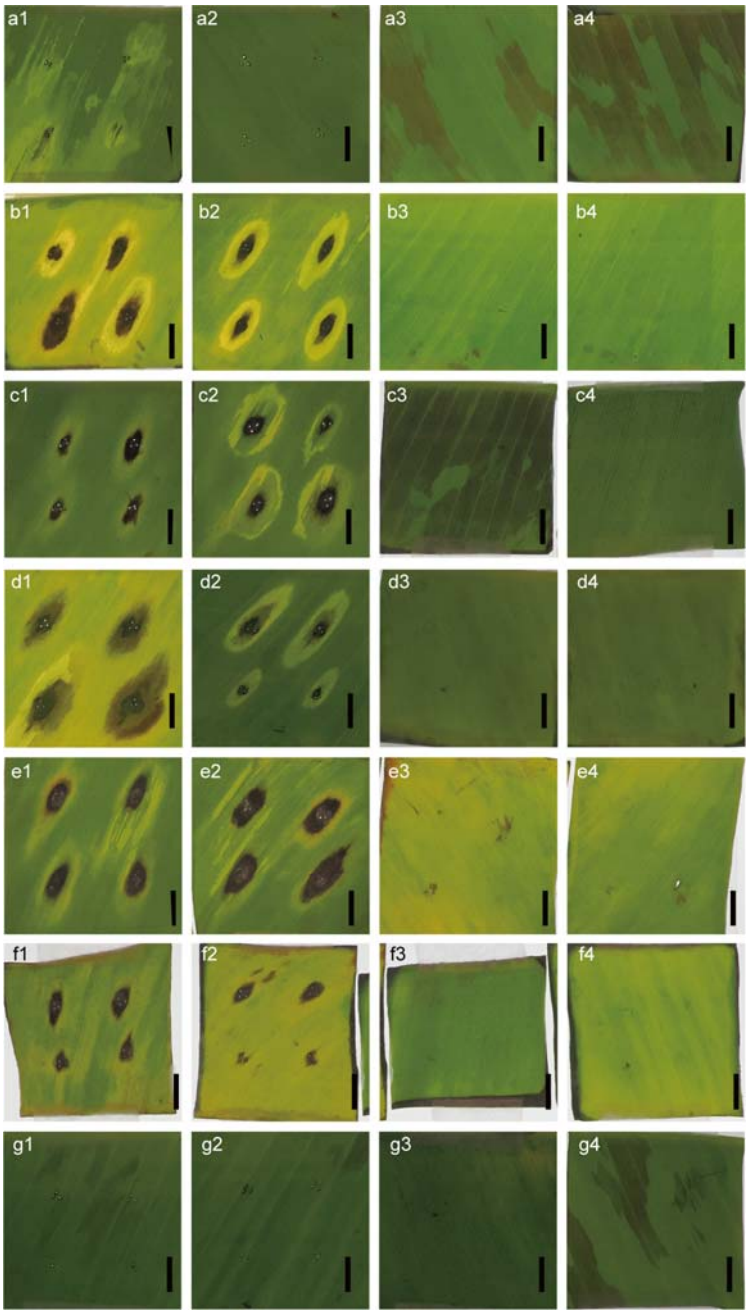

Fig. 10 Samples of banana leaves 4 days after inoculation with mycelial plugs. Inoculated leaves with *N. chinensis* (isolate TAP24N011) with wounds (a1, a2) and without wound (a3, a4), *N. lacticolonia* (isolate TAP24N078) with wounds (b1, b2) and without wound (b3, b4), *N. nigrocolonia* (isolate TAP24N237) with wounds (c1, c2) and without wound (c3, c4), *N.* cf. *singularis* (isolate TAP24N257) with wounds (d1, d2) and without wound (d3, d4), *N. sphaerica* (isolate TAP24N107) with wounds (e1, e2) and without wound (e3, e4), *N.vesicularifera* (isolate TAP24N023) with wounds (f1, f2) and without wound (f3, f4). Controls inoculated with potato dextrose agar discs with wounds (g1, g2) and without wound (g3, g4). Bars: 1 cm.

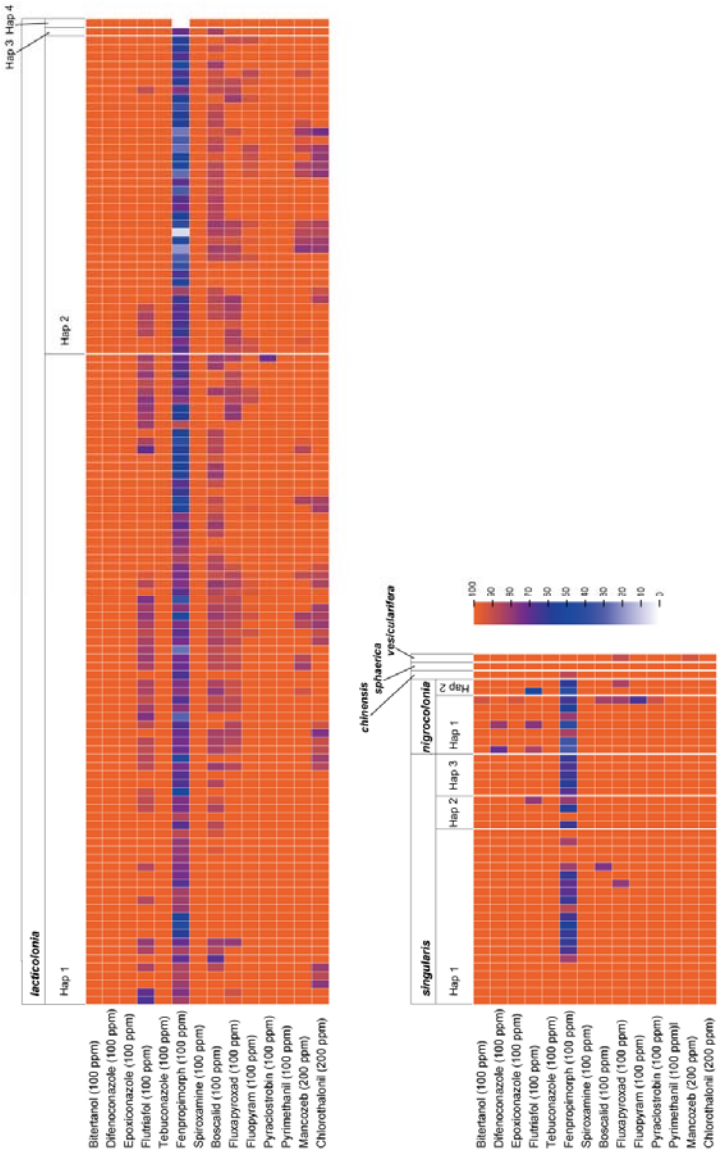

764 **Fig. 11 Heat map of the inhibition percentages for the isolates.**

765

766

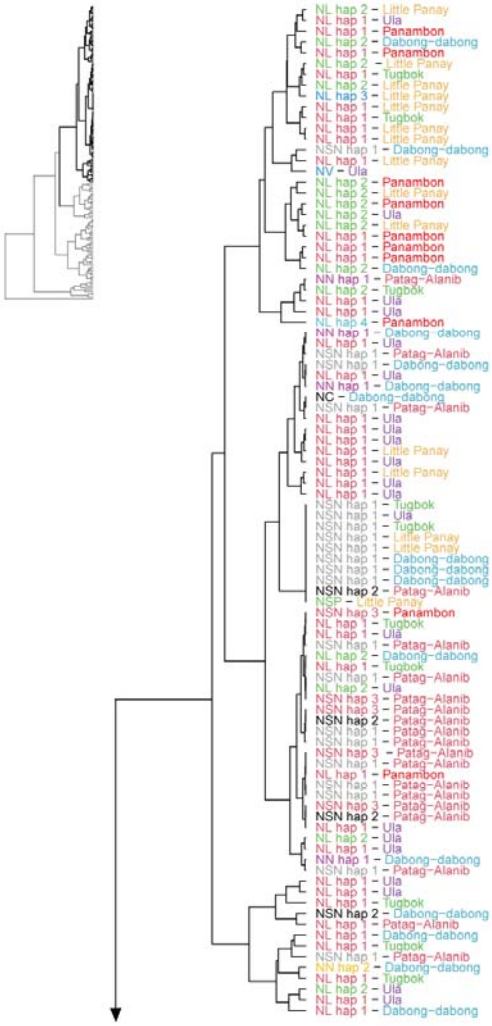

Fig. 12 Dendrogram based on coordinates on scatter plot of PCA derived from values of inhibition rates of fungicide. Label on the left and right of hyphen are species_haplotype and sampling site, respectively.

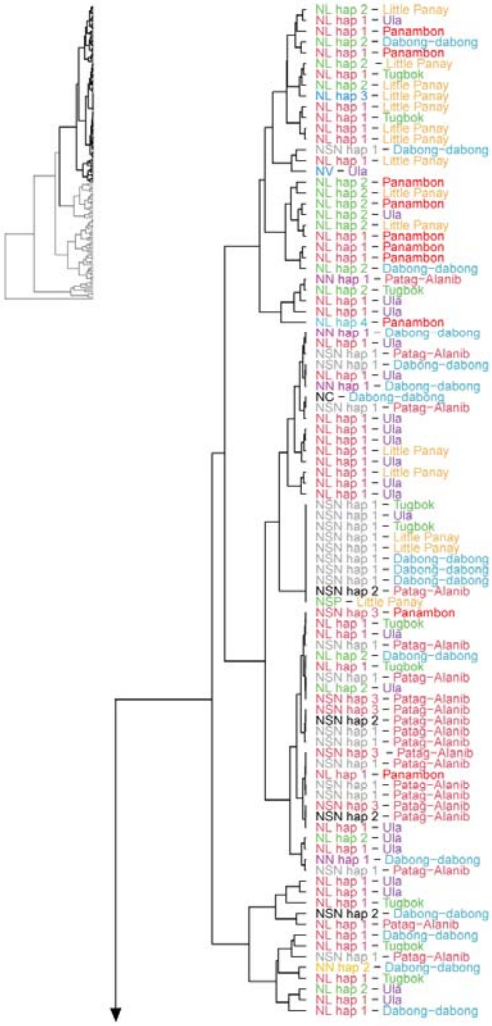

Fig. 12 Continued.

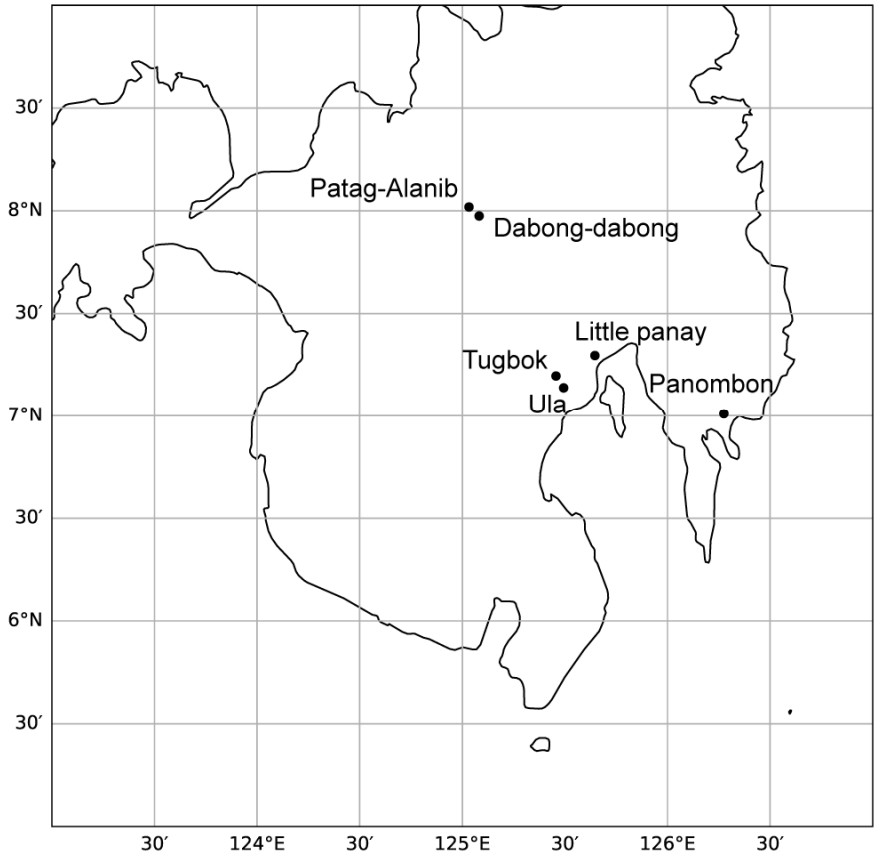

Fig. 13 Sampling sites in the Mindanao island, Philippines.

Table 1 Preliminary identification of 217 fungal isolates from banana leaf samples from six cities of Mindanao Island.

Genus[a]	Isolate numbers from different cities of Mindanao Island					
	Dabong-dabong	Little Panay	Panambon	Patag-Alanib	Tugbok	Ula
Alternaria	0	0	0	0	1	0
Annulohypoxylon	0	0	0	1	0	0
Colletotrichum	0	0	0	0	2	3
Curvularia	0	0	1	0	1	0
Dimorphiseta	0	0	1	0	0	0
Exserohilum	0	1	0	0	0	0
Fusarium	0	3	6	0	0	4
Lasiodiplodia	1	0	0	0	1	0
Microdochium	0	0	3	0	0	0
Musicillium	0	0	0	0	0	1
Mycosphaerella	0	1	0	0	0	0
Neosetophoma	0	2	3	0	0	0
Nigrospora	28	33	21	25	20	33
Ochrocladosporium	0	1	0	0	0	0
Phaeosphaeria	0	5	6	0	3	2
Preussia	0	0	0	1	0	0
Pseudopestalotiopsis	0	1	0	0	1	0
Zasmidium	0	0	0	0	0	1

[a]The fungal isolates were identified based on ITS sequences.

Table 2 Lesion length and virulence of isolates based on pathogenicity tests.

Species	Isolate	Lesion length (mm)	Virulence
N. chinensis	TAP24N249	0-3.39 (mean±sd = 0.42±0.42)	Weak
N. lacticolonia	TAP24N001	6.62-12.27 (mean±sd = 9.52±0.81)	Strong
	TAP24N003	0-12.7 (mean±sd = 8.25±1.33)	Strong
	TAP24N005	6.58-11.04 (mean±sd = 8.6±0.55)	Strong
	TAP24N006	5.17-10.99 (mean±sd = 8.67±0.67)	Strong
	TAP24N008	8.88-11.37 (mean±sd = 10.28±0.29)	Strong
	TAP24N010	5.93-9.59 (mean±sd = 8.09±0.48)	Strong
	TAP24N011	8.87-10.35 (mean±sd = 9.38±0.17)	Strong
	TAP24N012	7.94-11.95 (mean±sd = 10.12±0.49)	Strong
	TAP24N013	0-16.05 (mean±sd = 10.5±2.37)	Strong
	TAP24N014	0-6.81 (mean±sd = 2.94±0.94)	Weak
	TAP24N016	4.44-8.56 (mean±sd = 6.8±0.58)	Strong
	TAP24N017	2.87-9.1 (mean±sd = 5.49±0.75)	Moderate
	TAP24N018	8.18-14.24 (mean±sd = 11.14±0.74)	Strong
	TAP24N019	0-6.72 (mean±sd = 2.96±1)	Weak
	TAP24N021	2.33-9.37 (mean±sd = 5.8±0.82)	Moderate
	TAP24N022	0-10.48 (mean±sd = 5.97±1.2)	Moderate
	TAP24N026	4.12-11.74 (mean±sd = 7.44±0.75)	Strong
	TAP24N027	3.61-6.65 (mean±sd = 5.03±0.41)	Moderate
	TAP24N028	5.64-12.31 (mean±sd = 8.11±0.79)	Strong
	TAP24N029	0-5.88 (mean±sd = 4.43±0.69)	Moderate
	TAP24N030	5.1-9.27 (mean±sd = 6.66±0.52)	Strong
	TAP24N031	4.91-9.32 (mean±sd = 7.61±0.52)	Strong
	TAP24N033	3.36-13.2 (mean±sd = 7.9±1)	Strong
	TAP24N035	4.3-11.41 (mean±sd = 9.17±0.84)	Strong
	TAP24N036	9.39-13.93 (mean±sd = 11.7±0.5)	Strong
	TAP24N038	2.9-5.39 (mean±sd = 3.83±0.28)	Moderate
	TAP24N039	0-8.2 (mean±sd = 2.98±1.26)	Weak
	TAP24N041	0-4.51 (mean±sd = 0.94±0.63)	Weak
	TAP24N043	0-8.45 (mean±sd = 2.97±1.19)	Weak
	TAP24N045	0.11-7.3 (mean±sd = 4.28±0.8)	Moderate
	TAP24N047	0-9.55 (mean±sd = 4.89±1.06)	Moderate

TAP24N048	0-7.82 (mean±sd = 4.08±1.01)	Moderate
TAP24N050	0-4.35 (mean±sd = 1.38±0.68)	Weak
TAP24N053	3.31-9.21 (mean±sd = 5.81±0.64)	Moderate
TAP24N054	0-9.22 (mean±sd = 6.04±1.36)	Moderate
TAP24N055	0-7.07 (mean±sd = 2.23±1.12)	Weak
TAP24N057	0-6.09 (mean±sd = 2.67±1.03)	Weak
TAP24N060	0-10.81 (mean±sd = 7.43±1.24)	Strong
TAP24N062	4.89-8.56 (mean±sd = 6.74±0.48)	Strong
TAP24N063	0-10.13 (mean±sd = 4.09±1)	Moderate
TAP24N065	3.1-11.57 (mean±sd = 6.78±1.13)	Strong
TAP24N067	4.56-16.65 (mean±sd = 11.04±1.35)	Strong
TAP24N069	0-8.13 (mean±sd = 5.4±1.19)	Moderate
TAP24N071	3.13-6.88 (mean±sd = 4.92±0.41)	Moderate
TAP24N073	0-10.55 (mean±sd = 3.83±1.54)	Moderate
TAP24N074	0-5.44 (mean±sd = 2.26±0.9)	Weak
TAP24N077	4.17-10.38 (mean±sd = 7.12±0.61)	Strong
TAP24N078	5.19-20.07 (mean±sd = 12.31±1.54)	Strong
TAP24N079	0	Very weak
TAP24N082	6.81-11.43 (mean±sd = 8.89±0.62)	Strong
TAP24N085	2.69-11.25 (mean±sd = 5.93±1.13)	Moderate
TAP24N086	8.2-14.77 (mean±sd = 10.64±0.98)	Strong
TAP24N088	3.95-9.66 (mean±sd = 7.13±0.58)	Strong
TAP24N090	3.56-4.72 (mean±sd = 4.17±0.17)	Moderate
TAP24N091	0-5.5 (mean±sd = 1.51±0.79)	Weak
TAP24N092	0-9.04 (mean±sd = 5.44±1.03)	Moderate
TAP24N093	2.87-8.09 (mean±sd = 5.62±0.63)	Moderate
TAP24N094	5.19-14.99 (mean±sd = 8.22±1.09)	Strong
TAP24N095	5.88-11.22 (mean±sd = 7.54±0.66)	Strong
TAP24N096	0-7.13 (mean±sd = 2.99±0.97)	Weak
TAP24N098	5.64-15.34 (mean±sd = 9.94±1.42)	Strong
TAP24N099	4.44-9.75 (mean±sd = 7.05±0.75)	Strong
TAP24N100	4.7-9.72 (mean±sd = 6.76±0.63)	Strong
TAP24N101	4.47-11.81 (mean±sd = 7.85±0.83)	Strong
TAP24N102	3.56-11.43 (mean±sd = 7.38±1.25)	Strong
TAP24N103	5.3-11.07 (mean±sd = 7.87±0.71)	Strong

TAP24N104	0-10.43 (mean±sd = 7.55±1.17)	Strong
TAP24N105	0	non-pathogenic
TAP24N108	0-7.4 (mean±sd = 1.97±1.03)	Weak
TAP24N112	0-6.78 (mean±sd = 3.24±1.01)	Moderate
TAP24N113	0-5.89 (mean±sd = 3.48±0.84)	Moderate
TAP24N115	0-8.26 (mean±sd = 3.83±1)	Moderate
TAP24N118	0-7.31 (mean±sd = 3.08±1.07)	Moderate
TAP24N123	6.6-14.57 (mean±sd = 9.18±0.94)	Strong
TAP24N125	3.15-7.5 (mean±sd = 5.34±0.59)	Moderate
TAP24N127	2.95-8.03 (mean±sd = 6.15±0.69)	Moderate
TAP24N128	6.44-10.25 (mean±sd = 8.31±0.42)	Strong
TAP24N129	0-2.73 (mean±sd = 0.34±0.34)	Weak
TAP24N131	0-6.06 (mean±sd = 3.33±0.8)	Moderate
TAP24N132	0-5.39 (mean±sd = 2.44±0.67)	Weak
TAP24N134	0-5.47 (mean±sd = 2.75±0.66)	Weak
TAP24N136	0-7.98 (mean±sd = 4.5±0.95)	Moderate
TAP24N139	0-2.43 (mean±sd = 0.3±0.3)	Weak
TAP24N141	0-4.42 (mean±sd = 2.08±0.63)	Weak
TAP24N145	4.05-8.24 (mean±sd = 6.85±0.54)	Strong
TAP24N146	2.75-4.57 (mean±sd = 3.92±0.21)	Moderate
TAP24N149	3.39-6.56 (mean±sd = 4.82±0.36)	Moderate
TAP24N154	5.07-8.36 (mean±sd = 6.29±0.38)	Moderate
TAP24N156	3.72-9.3 (mean±sd = 6.19±0.68)	Moderate
TAP24N157	4.96-9 (mean±sd = 6.36±0.49)	Moderate
TAP24N163	6.19-9.6 (mean±sd = 7.54±0.35)	Strong
TAP24N164	2.72-9.06 (mean±sd = 5.02±0.75)	Moderate
TAP24N165	5.21-12.48 (mean±sd = 8.13±0.84)	Strong
TAP24N166	2.54-6.84 (mean±sd = 4.31±0.44)	Moderate
TAP24N167	2.57-5.46 (mean±sd = 4.12±0.42)	Moderate
TAP24N168	0-5.11 (mean±sd = 1.96±0.79)	Weak
TAP24N174	2.68-7.63 (mean±sd = 4.98±0.59)	Moderate
TAP24N176	4.12-12.73 (mean±sd = 7.87±1.25)	Strong
TAP24N177	5.11-9 (mean±sd = 7.14±0.54)	Strong
TAP24N204	0-5.1 (mean±sd = 3.11±0.71)	Moderate

	TAP24N208	3.11-7.33 (mean±sd = 4.13±0.51)	Moderate
	TAP24N209	0-4.82 (mean±sd = 2.81±0.68)	Weak
	TAP24N226	0-2.56 (mean±sd = 0.32±0.32)	Weak
	TAP24N230	6.43-22.2 (mean±sd = 12.78±1.94)	Strong
	TAP24N231	0	non-pathogenic
	TAP24N233	4.62-10.03 (mean±sd = 8.12±0.73)	Strong
	TAP24N234	0-3.27 (mean±sd = 0.81±0.53)	Weak
	TAP24N235	0	Very weak
	TAP24N236	0-3.26 (mean±sd = 0.41±0.41)	Weak
	TAP24N238	7.77-11.65 (mean±sd = 9.39±0.46)	Strong
	TAP24N239	0-6.58 (mean±sd = 4.23±0.76)	Moderate
	TAP24N240	2.38-7.19 (mean±sd = 4.91±0.57)	Moderate
	TAP24N242	6.09-9.67 (mean±sd = 8.41±0.48)	Strong
	TAP24N243	3.94-9.79 (mean±sd = 6.37±0.69)	Moderate
	TAP24N245	0-10.44 (mean±sd = 4.47±1.21)	Moderate
	TAP24N251	2.88-4.48 (mean±sd = 3.45±0.17)	Moderate
	TAP24N254	0	Very weak
	TAP24N255	4.07-8.51 (mean±sd = 5.82±0.58)	Moderate
N. nigrocolonia	TAP24N202	0-3.2 (mean±sd = 0.79±0.52)	Weak
	TAP24N222	2.84-5.92 (mean±sd = 3.87±0.4)	Moderate
	TAP24N224	0-6.34 (mean±sd = 3.18±0.72)	Moderate
	TAP24N229	0-5.95 (mean±sd = 3.02±0.8)	Weak
	TAP24N232	0	Very weak
	TAP24N237	6.8-10.9 (mean±sd = 8.69±0.61)	Strong
	TAP24N246	0-4.45 (mean±sd = 0.99±0.65)	Weak
	TAP24N250	0-5.67 (mean±sd = 0.71±0.71)	Weak
	TAP24N252	0-0.11 (mean±sd = 0.01±0.01)	Weak
N. cf. *singularis*	TAP24N034	0-5.34 (mean±sd = 0.67±0.67)	Weak
	TAP24N049	0-3.65 (mean±sd = 1.84±0.57)	Weak
	TAP24N068	4.05-12.2 (mean±sd = 6.5±0.9)	Moderate
	TAP24N081	4.84-13.4 (mean±sd = 8.14±1.08)	Strong
	TAP24N120	0-3.64 (mean±sd = 0.46±0.46)	Weak
	TAP24N137	0-2.75 (mean±sd = 0.86±0.43)	Weak
	TAP24N201	0-4.62 (mean±sd = 2.33±0.71)	Weak

	TAP24N203	0-4.33 (mean±sd = 1.86±0.73)	Weak
	TAP24N205	0-4.09 (mean±sd = 1.96±0.59)	Weak
	TAP24N206	0-4.04 (mean±sd = 3.07±0.46)	Weak
	TAP24N207	2.77-14.02 (mean±sd = 5.78±1.36)	Moderate
	TAP24N210	5.98-15.06 (mean±sd = 9.96±1.19)	Strong
	TAP24N211	0	Very weak
	TAP24N212	5.84-9.79 (mean±sd = 7.62±0.43)	Strong
	TAP24N213	0-4.54 (mean±sd = 2.86±0.47)	Weak
	TAP24N214	0-2.11 (mean±sd = 0.26±0.26)	Weak
	TAP24N215	0-4.08 (mean±sd = 2.42±0.53)	Weak
	TAP24N217	0	Very weak
	TAP24N218	3.73-8.67 (mean±sd = 6.11±0.63)	Moderate
	TAP24N219	3.24-6.9 (mean±sd = 5.57±0.45)	Moderate
	TAP24N220	0-3.43 (mean±sd = 1.9±0.53)	Weak
	TAP24N221	0-5.39 (mean±sd = 1.2±0.8)	Weak
	TAP24N223	0-6.24 (mean±sd = 2.41±1)	Weak
	TAP24N227	0	Very weak
	TAP24N241	0-16.05 (mean±sd = 8.12±1.89)	Strong
	TAP24N244	3.36-10.8 (mean±sd = 6.38±0.97)	Moderate
	TAP24N247	0-3.87 (mean±sd = 2.31±0.54)	Weak
	TAP24N248	0-5.58 (mean±sd = 3.1±0.75)	Moderate
	TAP24N256	0	Very weak
	TAP24N257	7.34-24.96 (mean±sd = 16.44±2.11)	Strong
N. sphaerica	TAP24N107	11.61-22.61 (mean±sd = 14.33±1.25)	Strong
N. vesicularifera	TAP24N023	0-10.51 (mean±sd = 7.8±1.25)	Strong

Aggressiveness was classified based on lesions as follows: strongly virulent (≥6.6 mm in mean length), moderately virulent (≥3 to <6.6 mm), weakly virulent (>0 to <3 mm), and very weakly virulent (0 mm with brown or yellow discoloration at or around the wound site).

779

Table 3 PCR conditions for amplifying ITS, *β-tubulin*, and *tef1α* regions.

Loci	Primer name	Reaction condition	Reference
ITS	ITS4 ITS5	94□, 3m; 94□, 60s, 55□, 60s, 72□, 60s, 35 cycles; 72□, 5m	White et al. 1990

β-tubulin	Bt2a Bt2b	94□, 3m; 94□, 1m, 50□, 1m, 72□, 60s, 35 cycles; 72□, 5m	Glass and Donaldson (1995)
Tef1α	Nigro_EF1 Nigro_EF2	94□, 3m; 94□, 30s, 60□, 30s, 72□, 60s; 30 cycles; 72□, 5m	This study

Table 4 GenBank accession numbers of the DNA sequences used in phylogenetic analysis and pathogenicity of our isolates.

Species	Isolates	Locations	GenBank accession no.		
			ITS	*β-tubulin*	*tef1a*
Apiospora malaysiana	CBS 102053	-	KF144896	KF144988	KF145030
A. pseudoparenchymatica	LC7234*	-	KY494743	KY705211	KY705139
Nigrospora aurantiaca	CGMCC 3.18130*	-	KX986064	KY019465	KY019295
N. aurantiaca	LC7034	-	KX986093	KY019598	KY019394
N. bambusae	CGMCC 3.18327*	-	KY385307	KY385319	KY385313
	LC7245	-	KY385305	KY385321	KY385315
N. brasiliensis	CMM 1214*	-	KY569629	MK720816	MK753271
	CMM 1217	-	KY569630	MK720817	MK753272
N. camelliae-sinensis	CGMCC 3.18125*	-	KX985986	KY019460	KY019293
N. chinensis	LC6851	-	KX986049	KY019579	KY019450
	CGMCC 3.18127*	-	KX986023	KY019462	KY019422
	TAP24N249	Dabong-dabong	**LC868051**	**LC868104**	**LC868157**
N. covidalis	CGMCC 3.20538*	-	OK335209	OK431479	OK431485
	LC158337	-	OK335210	OK431480	OK431486
	LC2725	-	KX985960	KY019487	KY019313
	LC4566	-	KX986022	KY019545	KY019354
N. endophytica	A.R.M. 687	-	OM265226	OP572418	OP572415
	A.R.M. 973*	-	OM265233	OP572420	OP572416
N. falsivesicularis	CGMCC 3.19678*	-	MN215778	MN329942	MN264017
	LC13553	-	MN215779	MN329943	MN264018
N. globospora	CGMCC 3.20539*	-	OK335211	OK431481	OK431487
	LC15839	-	OK335212	OK431482	OK431488
N. gorlenkoana	CBS 480.73*	-	KX986048	KY019456	KY019420
N. guangdongensis	CFCC:53917*	-	MT017509	MT024495	MT024493

N. guilinensis	LC7301	-	KX986063	KY019608	KY019404
	CGMCC 3.18124*	-	KX985983	KY019459	KY019292
N. hainanensis	CGMCC 3.18129*	-	KX986091	KY019464	KY019415
	A.R.M.967	-	OM265228	OM793057	OM642834
	A.R.M.968	-	OM265229	OM793058	OM642835
	A.R.M.972	-	OM265232	OP572419	OM642837
	A.R.M.976	-	OM265236	OM793060	OP572417
N. lacticolonia	CGMCC 3.18123*	-	KX985978	KY019458	KY019291
	A.R.M. 921	-	OM265227	OM642838	OM642833
	TAP24N001	Ula	**LC846677**	**LC846784**	**LC846891**
	TAP24N003	Ula	**LC846678**	**LC846785**	**LC846892**
	TAP24N005	Ula	**LC846679**	**LC846786**	**LC846893**
	TAP24N006	Ula	**LC846680**	**LC846787**	**LC846894**
	TAP24N008	Ula	**LC846681**	**LC846788**	**LC846895**
	TAP24N010	Ula	**LC846682**	**LC846789**	**LC846896**
	TAP24N011	Ula	**LC846683**	**LC846790**	**LC846897**
	TAP24N012	Ula	**LC846684**	**LC846791**	**LC846898**
	TAP24N013	Ula	**LC846685**	**LC846792**	**LC846899**
	TAP24N014	Ula	**LC846686**	**LC846793**	**LC846900**
	TAP24N016	Ula	**LC846687**	**LC846794**	**LC846901**
	TAP24N017	Ula	**LC846688**	**LC846795**	**LC846902**
	TAP24N018	Ula	**LC846689**	**LC846796**	**LC846903**
	TAP24N019	Ula	**LC846690**	**LC846797**	**LC846904**
	TAP24N021	Ula	**LC846691**	**LC846798**	**LC846905**
	TAP24N022	Ula	**LC846692**	**LC846799**	**LC846906**
	TAP24N026	Ula	**LC846694**	**LC846801**	**LC846908**
	TAP24N027	Ula	**LC846695**	**LC846802**	**LC846909**
	TAP24N028	Ula	**LC846696**	**LC846803**	**LC846910**
	TAP24N029	Ula	**LC846697**	**LC846804**	**LC846911**
	TAP24N030	Ula	**LC846698**	**LC846805**	**LC846912**
	TAP24N031	Ula	**LC846699**	**LC846806**	**LC846913**
	TAP24N033	Ula	**LC846700**	**LC846807**	**LC846914**
	TAP24N035	Ula	**LC846702**	**LC846809**	**LC846916**
	TAP24N036	Ula	**LC846703**	**LC846810**	**LC846917**
	TAP24N038	Ula	**LC846704**	**LC846811**	**LC846918**
	TAP24N039	Ula	**LC846705**	**LC846812**	**LC846919**
	TAP24N041	Ula	**LC846706**	**LC846813**	**LC846920**
	TAP24N043	Ula	**LC846707**	**LC846814**	**LC846921**
	TAP24N045	Ula	**LC846708**	**LC846815**	**LC846922**
	TAP24N047	Ula	**LC846709**	**LC846816**	**LC846923**
	TAP24N048	Tugbok	**LC846710**	**LC846817**	**LC846924**
	TAP24N050	Tugbok	**LC846712**	**LC846819**	**LC846926**

TAP24N053	Tugbok	**LC846713**	**LC846820**	**LC846927**
TAP24N054	Tugbok	**LC846714**	**LC846821**	**LC846928**
TAP24N055	Tugbok	**LC846715**	**LC846822**	**LC846929**
TAP24N057	Tugbok	**LC846716**	**LC846823**	**LC846930**
TAP24N060	Tugbok	**LC846717**	**LC846824**	**LC846931**
TAP24N062	Tugbok	**LC846718**	**LC846825**	**LC846932**
TAP24N063	Tugbok	**LC846719**	**LC846826**	**LC846933**
TAP24N065	Tugbok	**LC846720**	**LC846827**	**LC846934**
TAP24N067	Tugbok	**LC846721**	**LC846828**	**LC846935**
TAP24N069	Tugbok	**LC846723**	**LC846830**	**LC846937**
TAP24N071	Tugbok	**LC846724**	**LC846831**	**LC846938**
TAP24N073	Tugbok	**LC846725**	**LC846832**	**LC846939**
TAP24N074	Tugbok	**LC846726**	**LC846833**	**LC846940**
TAP24N077	Tugbok	**LC846727**	**LC846834**	**LC846941**
TAP24N078	Tugbok	**LC846728**	**LC846835**	**LC846942**
TAP24N079	Tugbok	**LC846676**	**LC846783**	**LC846890**
TAP24N082	Little Panay	**LC846730**	**LC846837**	**LC846944**
TAP24N085	Little Panay	**LC846731**	**LC846838**	**LC846945**
TAP24N086	Little Panay	**LC846732**	**LC846839**	**LC846946**
TAP24N088	Little Panay	**LC846733**	**LC846840**	**LC846947**
TAP24N090	Little Panay	**LC846734**	**LC846841**	**LC846948**
TAP24N091	Little Panay	**LC846735**	**LC846842**	**LC846949**
TAP24N092	Little Panay	**LC846736**	**LC846843**	**LC846950**
TAP24N093	Little Panay	**LC846737**	**LC846844**	**LC846951**
TAP24N094	Little Panay	**LC846738**	**LC846845**	**LC846952**
TAP24N095	Little Panay	**LC846739**	**LC846846**	**LC846953**
TAP24N096	Little Panay	**LC846740**	**LC846847**	**LC846954**
TAP24N098	Little Panay	**LC846741**	**LC846848**	**LC846955**
TAP24N099	Little Panay	**LC846742**	**LC846849**	**LC846956**
TAP24N100	Little Panay	**LC846743**	**LC846850**	**LC846957**
TAP24N101	Little Panay	**LC846744**	**LC846851**	**LC846958**
TAP24N102	Little Panay	**LC846745**	**LC846852**	**LC846959**

TAP24N103	Little Panay	**LC846746**	**LC846853**	**LC846960**
TAP24N104	Little Panay	**LC846747**	**LC846854**	**LC846961**
TAP24N105	Little Panay	**LC846748**	**LC846855**	**LC846962**
TAP24N108	Little Panay	**LC846750**	**LC846857**	**LC846964**
TAP24N112	Little Panay	**LC846751**	**LC846858**	**LC846965**
TAP24N113	Little Panay	**LC846752**	**LC846859**	**LC846966**
TAP24N115	Little Panay	**LC846753**	**LC846860**	**LC846967**
TAP24N118	Little Panay	**LC846754**	**LC846861**	**LC846968**
TAP24N123	Little Panay	**LC846756**	**LC846863**	**LC846970**
TAP24N125	Little Panay	**LC846757**	**LC846864**	**LC846971**
TAP24N127	Little Panay	**LC846758**	**LC846865**	**LC846972**
TAP24N128	Little Panay	**LC846759**	**LC846866**	**LC846973**
TAP24N129	Little Panay	**LC846760**	**LC846867**	**LC846974**
TAP24N131	Little Panay	**LC846761**	**LC846868**	**LC846975**
TAP24N132	Panombon	**LC846762**	**LC846869**	**LC846976**
TAP24N134	Panombon	**LC846763**	**LC846870**	**LC846977**
TAP24N136	Panombon	**LC846764**	**LC846871**	**LC846978**
TAP24N139	Panombon	**LC846766**	**LC846873**	**LC846980**
TAP24N141	Panombon	**LC846767**	**LC846874**	**LC846981**
TAP24N145	Panombon	**LC846768**	**LC846875**	**LC846982**
TAP24N146	Panombon	**LC846769**	**LC846876**	**LC846983**
TAP24N149	Panombon	**LC846770**	**LC846877**	**LC846984**
TAP24N154	Panombon	**LC846771**	**LC846878**	**LC846985**
TAP24N156	Panombon	**LC846772**	**LC846879**	**LC846986**
TAP24N157	Panombon	**LC846773**	**LC846880**	**LC846987**
TAP24N163	Panombon	**LC846774**	**LC846881**	**LC846988**
TAP24N164	Panombon	**LC846775**	**LC846882**	**LC846989**
TAP24N165	Panombon	**LC846776**	**LC846883**	**LC846990**
TAP24N166	Panombon	**LC846777**	**LC846884**	**LC846991**
TAP24N167	Panombon	**LC846778**	**LC846885**	**LC846992**
TAP24N168	Panombon	**LC846779**	**LC846886**	**LC846993**
TAP24N174	Panombon	**LC846780**	**LC846887**	**LC846994**
TAP24N176	Panombon	**LC846781**	**LC846888**	**LC846995**
TAP24N177	Panombon	**LC846782**	**LC846889**	**LC846996**

	TAP24N204	Patag-Alanib	**LC868092**	**LC868145**	**LC868198**
	TAP24N208	Patag-Alanib	**LC868088**	**LC868141**	**LC868194**
	TAP24N209	Patag-Alanib	**LC868087**	**LC868140**	**LC868193**
	TAP24N226	Patag-Alanib	**LC868097**	**LC868150**	**LC868203**
	TAP24N230	Dabong-dabong	**LC868070**	**LC868123**	**LC868176**
	TAP24N231	Dabong-dabong	**LC868069**	**LC868122**	**LC868175**
	TAP24N233	Dabong-dabong	**LC868067**	**LC868120**	**LC868173**
	TAP24N234	Dabong-dabong	**LC868066**	**LC868119**	**LC868172**
	TAP24N235	Dabong-dabong	**LC868065**	**LC868118**	**LC868171**
	TAP24N236	Dabong-dabong	**LC868064**	**LC868117**	**LC868170**
	TAP24N238	Dabong-dabong	**LC868062**	**LC868115**	**LC868168**
	TAP24N239	Dabong-dabong	**LC868061**	**LC868114**	**LC868167**
	TAP24N240	Dabong-dabong	**LC868060**	**LC868113**	**LC868166**
	TAP24N242	Dabong-dabong,	**LC868058**	**LC868111**	**LC868164**
	TAP24N243	Dabong-dabong	**LC868057**	**LC868110**	**LC868163**
	TAP24N245	Dabong-dabong	**LC868055**	**LC868108**	**LC868161**
	TAP24N251	Dabong-dabong	**LC868049**	**LC868102**	**LC868155**
	TAP24N254	Dabong-dabong	**LC868047**	**LC868100**	**LC868153**
	TAP24N255	Dabong-dabong	**LC868046**	**LC868099**	**LC868152**
N. manihoticola	A.R.M. 645*	-	OM265224	OM869479	OM914791
N. musae	CBS 319.34*	-	KX986076	KY019455	KY019419
	LC6385	-	KX986042	KY019567	KY019371
N. nigrocolonia	**TAP24N202**	Patag-Alanib	**LC868094**	**LC868147**	**LC868200**
	TAP24N222	Patag-Alanib	**LC868075**	**LC868128**	**LC868181**
	TAP24N224	Patag-Alanib	**LC868073**	**LC868126**	**LC868179**
	TAP24N229	Dabong-dabong	**LC868071**	**LC868124**	**LC868177**
	TAP24N232	Dabong-dabong	**LC868068**	**LC868121**	**LC868174**

	TAP24N237	Dabong-dabong	**LC868063**	**LC868116**	**LC868169**
	TAP24N246	Dabong-dabong	**LC868054**	**LC868107**	**LC868160**
	TAP24N250	Dabong-dabong	**LC868050**	**LC868103**	**LC868156**
	TAP24N252	Dabong-dabong	**LC868048**	**LC868101**	**LC868154**
N. oryzae	LC2724	-	KX985959	KY019486	KY019312
	LC4265	-	KX985994	KY019518	KY019335
N. osmanthi	CGMCC 3.18126*	-	KX986010	KY019461	KY019421
	LC4487	-	KX986017	KY019540	KY019438
N. pernambucoensis	A.R.M.651	-	OM265225	OM869480	OM914792
	A.R.M. 974*	-	OM265234	OM869481	OM914793
N.philosophiae-doctoris	CGMCC 3.20540*	-	OK335214	OK431484	OK431490
N. pyriformis	CGMCC 3.18122*	-	KX985940	KY019457	KY019290
	A.R.M.970	-	OM265231	OM642839	OM513904
N. rubi	LC2698*	-	KX985948	KY019475	KY019302
N. saccharicola	LC12057	-	MN215789	MN329952	MN264028
	CGMCC 3.19362*	-	MN215788	MN329951	MN264027
N. sacchari-officinarum	CGMCC 3.19335*	-	MN215791	MN329954	MN264030
	LC13531	-	MN215792	MN329955	MN264031
N. singularis	CGMCC 3.19334*	-	MN215793	MN329956	MN264032
	LC12068	-	MN215794	MN329957	MN264033
	TAP24N034	Ula	**LC846701**	**LC846808**	**LC846915**
	TAP24N049	Tugbok	**LC846711**	**LC846818**	**LC846925**
	TAP24N068	Tugbok	**LC846722**	**LC846829**	**LC846936**
	TAP24N081	Little Panay	**LC846729**	**LC846836**	**LC846943**
	TAP24N120	Little Panay	**LC846755**	**LC846862**	**LC846969**
	TAP24N137	Panombon	**LC846765**	**LC846872**	**LC846979**
	TAP24N201	Patag-Alanib	**LC868095**	**LC868148**	**LC868178**
	TAP24N203	Patag-Alanib	**LC868093**	**LC868146**	**LC868199**
	TAP24N205	Patag-Alanib	**LC868091**	**LC868144**	**LC868197**
	TAP24N206	Patag-Alanib	**LC868090**	**LC868143**	**LC868196**
	TAP24N207	Patag-Alanib	**LC868089**	**LC868142**	**LC868195**
	TAP24N210	Patag-	**LC868086**	**LC868139**	**LC868192**

		Alanib			
	TAP24N211	Patag-Alanib	**LC868085**	**LC868138**	**LC868191**
	TAP24N212	Patag-Alanib	**LC868084**	**LC868137**	**LC868190**
	TAP24N213	Patag-Alanib	**LC868083**	**LC868136**	**LC868189**
	TAP24N214	Patag-Alanib	**LC868082**	**LC868135**	**LC868188**
	TAP24N215	Patag-Alanib	**LC868081**	**LC868134**	**LC868187**
	TAP24N217	Patag-Alanib	**LC868080**	**LC868133**	**LC868186**
	TAP24N218	Patag-Alanib	**LC868079**	**LC868132**	**LC868185**
	TAP24N219	Patag-Alanib	**LC868078**	**LC868131**	**LC868184**
	TAP24N220	Patag-Alanib	**LC868077**	**LC868130**	**LC868183**
	TAP24N221	Patag-Alanib	**LC868076**	**LC868129**	**LC868182**
	TAP24N223	Patag-Alanib	**LC868074**	**LC868127**	**LC868180**
	TAP24N227	Patag-Alanib	**LC868063**	**LC868125**	**LC868178**
	TAP24N241	Dabong-dabong	**LC868059**	**LC868112**	**LC868165**
	TAP24N244	Dabong-dabong	**LC868056**	**LC868109**	**LC868162**
	TAP24N247	Dabong-dabong	**LC868053**	**LC868106**	**LC868159**
	TAP24N248	Dabong-dabong	**LC868052**	**LC868105**	**LC868158**
	TAP24N256	Dabong-dabong	**LC868096**	**LC868149**	**LC868202**
	TAP24N257	Dabong-dabong	**LC868045**	**LC868098**	**LC868151**
N. sphaerica	LC2839	-	KX985964	KY019491	KY019317
	LC2840	-	KX985965	KY019492	KY019318
	TAP24N107	Little Panay	**LC846749**	**LC846856**	**LC846963**
Nigrospora sp.	LC6704	-	KX986047	KY019571	KY019373
N. vesicularis	LC0322	-	KX985939	KY019467	KY019296
	CGMCC 3.18128*	-	KX986088	KY019463	KY019294
N. vesicularifera	CGMCC 3.19333*	-	MN215812	MN329975	MN264051
	A.R.M.975	-	OM265235	OM642840	OM513905
N. vesicularifera	**TAP24N023**	Ula	**LC846693**	**LC846800**	**LC846907**
N. zimmermanii	CBS 290.62*	-	KY385309	KY385317	KY385311

	CBS 984.69	-	KY385310	KY385322	KY385316

782